FEED-FORWARD THALAMIC MODULATION AND NEUROPLASTICITY IN THE AUDITORY CORTEX

Yu Kai

Ph.D

The Hong Kong Polytechnic University

2013

The Hong Kong Polytechnic University

Department of Rehabilitation Sciences

Feed-forward thalamic modulation and neuroplasticity in the auditory cortex

Yu Kai

A thesis submitted in partial fulfillment of the requirements for the degree of Doctor of Philosophy

December 2012

CERTIFICATE OF ORIGINALITY

I hereby declare that this thesis is my own work and that, to the best of my knowledge and belief, it reproduces no material previously published or written, nor material that has been accepted for the award of any other degree or diploma, except where due acknowledgement has been made in the text.

_____ (Signature of Candidate)

Yu Kai (Name of Candidate)

_____ (Date)

Abstract

Auditory signals sensed by the hair cells pass through many relay stages in the auditory pathway. The signals are segregated and modulated at all the relay stages. At the last relay before reaching to the auditory cortex, signals are segregated in the medial geniculate body (MGB) into three divisions: the ventral (MGv), the dorsal (MGd), and the medial (MGm) divisions. We paid attention to the anatomical differences between the MGv and MGm. Firstly, the MGv projects very focally to the primary auditory cortex, while the MGm projects greatly to entire auditory cortex and beyond. Secondly, comparing with the uniformly shaped MGv neurons, neurons in MGm have varied shapes from small to giant. The MGm is also called the magnocellular nucleus. Thirdly, the MGv projects to layers III and IV in the cortex, while the MGm projects to layers I and VI. It is interesting to note that many MGm neurons show the shortest response latency to the auditory stimuli in the MGB. The first question of the present study was what the fast signals from giant cells in the MGm do in the auditory cortex.

We hypothesized that the MGm has a feed-forward modulation of the neuronal response to the later coming signals from the MGv in the auditory cortex. As the MGm projects to the superficial layer, we ask the second question: how the superficial layer neurons modulate the neuronal activities in other layers?

In the present study, we examined neuronal responses to the auditory stimuli in the auditory cortex of the anaesthetized guinea pig, with combination intracellular and extracellular recordings. The MGm or MGv was reversibly inactivated with local application of lidocaine.

The firing mode of cortical neurons in responses to acoustic stimuli was changed after the MGm was reversibly inactivated. However, the inactivation of MGv totally abolished the neuronal responses in the auditory cortex. Each auditory

stimulus with the inter-stimulus interval (ISI) of 3s evoked an oscillatory response in the auditory cortex, when the MGm was intact. The same stimulus became less capable in triggering the oscillatory response when the MGm was inactivated. The latency of the onset excitatory post-synaptic potential (EPSP) auditory response increased after the MGm was inactivated. Electrical activation of a small region of the superficial layer neurons of the auditory cortex caused a change in the state of spontaneous neuronal responses from slow oscillatory mode to tonic mode. Activation of single neuron in the superficial layer also caused a change in the state of the spontaneous activities of the activated neuron, the neighboring neurons in different layers with extracellular recording, and even in the field potential in a distant (> 2 mm) electrode.

Putting the above results together, we concluded that the fast responding giant MGm neurons placed a strong feed-forward modulatory effect on the auditory cortex through their projection to the superficial layer. The modulation was wide-spread in the auditory cortex and possible beyond the auditory modality.

In the next part of the study, we focused on the neuronal plasticity in the auditory cortex. The plasticity of synapse is widely accepted as a candidate mechanism of learning and memory in the brain. From the first published long term potentiation (LTP) induction experiment by Tim Bliss and colleagues in 1972, most experimenters have induced LTP through high frequency or repeated stimuli. Such artificial stimulus patterns in the experimental preparation are, however, uncommon in natural condition. The hippocampus is widely believed to serve only as a memory buffer instead of the location to store permanent memory. The cerebral cortex is regarded as the site for long term memory storage. In a parallel study by Chen and colleagues in our laboratory, they have found that an artificial visuoauditory memory trace could be induced in the auditory cortex through conditioning a combined stimulus of electrical stimulation of the auditory cortex and a visual stimulus with foot shock in the

behaving rat. The auditory cortex started to respond to the visual stimulus after some 20 trials conditioning. However, the induction was blocked after drug inactivation of the entorhinal cortex of the medial temporal lobe. A further parallel study in our lab has revealed that the projection neurons from the entorhinal cortex to the auditory cortex were cholecystokinin (CCK) neurons and inactivation of the CCK receptors in the auditory cortex blocked the above artificial visuoauditory memory traces in the auditory cortex, similar to the experiment of the inactivation of the entorhinal cortex.

We hypothesized that the plasticity in the auditory cortex needed the presence of CCK. In the following study, we first used the in-vivo intracellular recording technique to examine neurons in the auditory cortex to see if they could change their responses to the auditory or visual stimuli after pairing of the conditioned stimulus with depolarization of the recorded neurons. Spikes were triggered by the depolarized current.

The EPSP response to the conditioned auditory stimulus was potentiated from 3.9±1.6 to 5.1±1.7 mV at 4 min after the 2-trial pairings of the presynaptic input and postsynaptic firing in the presence of CCK ($P<0.01$, $n=14$, paired student t-test). The potentiation lasted as long as the recording was kept from 10min to 110min. No synaptic potentiation was observed (1) after simultaneous co-occurrence of pre- and postsynaptic activities, but without the local application of CCK in the auditory cortex, (2) after only presynaptic activity in the presence of CCK, and (3) after only postsynaptic firings in the presence of CCK. The auditory neurons started to response to the visual stimulus after it was paired with the depolarization for 40 trials ($n=2$). In the presence of CCK, the neurons in the auditory cortex changed their responses to the conditioned electrical stimulation in the nearby cortex but not to that at the control site, where no conditioning was made.

In the following in vitro experiment, we investigated the temporal relationship between the CCK receptor activation and neuronal plasticity

postsynaptically. We adopted the patch-clamp technique on cultured cortical neurons of the rat. Pairing of a simultaneous puffing of CCK and glutamate and the depolarization of the neuron did not induce change in the neural response to the glutamate puffing. When the puffing of CCK advanced the puffing of glutamate by 20 to 90s (20, 60, and 90s) in the pairing, potentiation in the EPSP to glutamate puffing was achieved. When the interval between the puffs of CCK and glutamate was further prolonged to 120s, no potentiation was observed.

In summary of the second part, neuroplasticity could happen in the auditory cortex of the anaesthetized guinea pig in the presence of CCK. The CCK receptors had to be activated earlier than the pre- and post-synaptic co-activities in 20-90s, in order to produce synaptic plasticity change of neuron.

Relevant Publications

Journal Papers in submission:

1. Xiao Li, Kai Yu, Zicong Zhang, Wen-Jian Sun, Zhou Yang, Chun-Hua Liu, HaitaoWang, Xi Chen, Yi Ping Guo, and Jufang He. Cholecystokinin: A Memory-Writing Chemical in the Neocortex

2. Haitao Wang, Jia Tang, Kai Yu, Joey Zhou Yang, and Jufang He. Single-trial pairing of glutamate-puff and postsynaptic firing in the presence of cholecystokinin produces synaptic potentiation

Conference paper:

Kai Yu, Jufang He (2011) Superficial layer neurons modulates the oscillation states of the auditory cortex. *Society for Neuroscience 41th Annual Meeting Washington DC, United States, November 11-15, 2011*

Acknowledgement:

I want to begin by profusely thanking Prof. Jufang He, for his patient guidance and great support in the past few years. Knowledge and experimental skills learnt from Prof. He's lab will be beneficial through the years. The straight-forward methodology , strong confidence in research work and being optimistic to the feedback left a deep impression and made a model of lifelong learning for us.

I also would like to express my sincere appreciation to my dear wife. She is always showing patience and unreserved support to my study and research work.

I thank my parents for giving me life and chance to explore such a wonderful world.

Finally, I would like to take the opportunity to thank all the members including several left before, thanks for enjoying these years together in Hong Kong.

Table of Contents

List of Figures

List of abbreviations

AC: auditory cortex

- AAF: anterior auditory field
- AI: Primary auditory field
- AII: secondary auditory cortical field
- DC: dorsocaudal belt
- DCB: dorsocardal belt
- DRB: dorsorostral belt
- S: small field
- VCB: ventrocaudal belt
- VRB: ventrorostral belt

AMPA: 2-amino-3-(3-hydroxy-5-methyl-isoxazol-4-yl) propanoic acid

AP: Action potential

CCK: Cholecystokinin

- CCK8s: Sulfated Cholecystokinin octapeptide

CCKR: Cholecystokinin receptor

- CCKRA: Cholecystokinin receptor type A
- CCKRB: Cholecystokinin receptor type B

CF: characteristic frequency

CT: corticothalamic

EC: Entorhinal cortex

EPSP: excitatory postsynaptic potential

ES: Electrical stimulation

Ex: Extracellular Recording

GABA: γ-aminobutyric acid

IC: inferior colliculus

i.p.: intraperitoneal

Intra: Intracellular recording

IPSP: inhibitory postsynaptic potential

ISI: inter-stimulus interval

LGN: lateral geniculate nucleus

LTS: low threshold calcium spikes

LTP: Long term potentiation

MGB: medial geniculate body

- MGd: dorsal nucleus
- MGm: medial nucleus
- MGv: ventral nucleus

NMDA:

SC: superior colliculus

SPL: sound pressure level

TRN: thalamic reticular nucleus

TC: thalamocortical

Vm: membrane potential

Chapter 1 Introduction

1.1 Background of the study

In mammals, the cerebral cortex is a main center of information processing and storage. From the hair cells of the cochlea to the auditory cortex, there are at least seven defined stages in the auditory pathway. Auditory signals are segregated and modulated at every stage (Popper and Fay 1992). The last stage before the cortex is the medial geniculate body (MGB). The MGB is divided into three parts based on cytoarchitecture and projection patterns; these three divisions are the ventral (MGv), dorsal (MGd), and medial (MGm) (Winer 1985; Webster, Popper et al. 1992). The MGv carries the main stream of auditory information. It receives projections mainly from the inferior colliculus (IC) and thalamic reticular nucleus (RTN). Neurons in the MGv share uniform properties, including morphology, sharp tuning curves, and organized ascending parallel projections to layer III/IV of the primary auditory cortex(Winer 1984). Neurons in the MGm have sizes that vary from small to giant. Projections to the MGm have various origins. In addition to the IC, the MGm also receives input from the dorsal cochlear nucleus, other brainstem auditory nuclei, the spinal cord, the vestibular nucleus, and the superior colliculus. The primary cortical projection of the MGm arrives at layer I and distributes to all auditory fields and beyond. Layer I of the auditory cortex is rich in neurpil development and contains few neurons. The axons from the MGm are the largest axonal trunks in Layer I and run laterally for a long distance in the auditory cortex (Sousa-Pinto, Paula-Barbosa et al. 1975; Winer 1986; Winer and Larue 1989). The large projection field of the MGm suggests poor selectivity over auditory signals and global influence over cortical neurons.

Although researchers have long been aware of the anatomical differences between the MGv and MGm, the functional differences remain largely unclear. Previous studies performed in our laboratory suggest that there are two parallel

ascending pathways from the thalamus to the cortex, and this assertion is consistent with the results from some other researchers. Additionally, it is interesting to note that some neurons in the MGm have the shortest response latencies to auditory stimuli in the MGB. The hypothesis that, in contrast to the direct relay function of the MGv, the MGm has a feed-forward modulatory effect on neurons in the auditory cortex and this modulation effect has a global impact on all auditory fields has been offered. Examination of the changes in the responses of cortical neurons to manipulation of the MGm and its downstream targets should provide us a chance to test this hypothesis.

In addition to its information processing functions, the auditory cortex also contributes to auditory learning and memory. For a long time, studies of learning and memory have focused on the hippocampus or surrounding structures. Based on the studies of the famous patient H.M., the hippocampus was identified as a key structure in learning and memory but not as the ultimate site of long-term memory storage. H.M. showed the capacity to recall remote memories that occurred before bilateral hippocampus ablation. However, H.M. did suffer a certain extent of retrograde amnesia; he did not have memories for a period of several years before the surgery. Some researchers have suggested that the hippocampus might serve as a buffer that holds memories for a short period of time; these memories are then downloaded to the cortex for long-term storage. However, direct experimental evidence supporting this hypothesis is lacking.

On the other hand, LTP is a possible cellular mechanism underlying long-term memory and has been extensively studied. In 1973, Tim Bliss and colleagues demonstrated LTP in both anaesthetized and unanaesthetized rabbits. A large number of subsequent experiments have shown that LTP is a universal phenomenon across the nervous systems of various animal models and different preparations. This evidence has made LTP the most likely candidate for learning and memory. However, in most of these experiments, LTP has been induced with high frequency or multiple repeated stimuli; these thresholds of induction are not common in nature. This fact creates

problems for the application of the popular model of LTP induction to the real world. Additionally, LTP models based on in vitro experiments neglect the contribution of modulatory systems that have prominent influences in adjusting brain function. Animals show impairment of learning and memory when the modulatory pathways are inactivated. CCK is known as a neural modulator and is highly expressed in the hippocampus. In many behavioral studies, CCK has been shown to impact learning and memory. Investigation of the mechanisms by which CCK contributes to memory function and investigations of the role of CCK in LTP induction should help our understanding of the secrets of memory.

1.2 Aims of the study

In general, the goal of the present study is to enrich our knowledge about how auditory information is processed and stored in the brain.

The first specific aim of this study was to investigate the feed-forward modulation effect of the MGm on the auditory cortex. Using in vivo intracellular and extracellular recordings in the auditory cortex combined with inactivation of MGm by local drug administration, we compared responses to acoustic stimuli in the auditory cortex with or without MGm inputs.

The second specific aim of this study was to examine the possible mechanism underlying the global modulation effect of the MGm in the auditory cortex. The superficial layer is one of the targets of MGm projections, and we investigated the influences of manipulation of a single or a small group of superficial cortical neurons on the changing states of neurons in a large cortical area.

The third specific aim of this study was to examine whether CCK facilitates LTP induction in cortical neurons in vivo.

The fourth specific aim was to investigate the mechanism underlying facilitation of LTP induction in cortical neurons by CCK. We conducted experiments in isolated cortical neuron cultures. The effective action time window was examined by changing CCK puffing times before the LTP induction process.

1.3 Significance of the study

In the first part of the present study, we show a significant modulating effect of the MGm on the auditory cortex. The properties of this modulation were further analyzed. Based on the present results and previous findings, we propose a feed-forward modulation model.

In the second part of this study, we successfully produced LTP using a few conditioned paired stimuli. The facilitating effect of CCK on LTP was tested in an in vivo preparation. In contrast to popular experiment paradigms, the threshold for inducing LTP was much easier to reach. This type of LTP is a more likely candidate mechanism for long-term memory formation in the neocortex. The effective action time window of CCK provided a clue for investigating its underlying mechanism. The working model in which CCK switches long-term memory formation to the cortex provided new insight into the mechanism of memory in the brain.

1.4 Thesis outline

Chapter 1 introduces the background of the present study. The objectives and significance of the study are also included.

Chapter 2 provides a comprehensive literature review on the topics of the present study and includes information about the current knowledge of the anatomy of the auditory system, the hippocampal system, the modulatory function of the thalamocortical system and current understanding of learning and memory.

Chapter 3 lists the methods used in the experiments including experimental data acquisition and processing.

Chapter 4 describes the results demonstrating the MGm's feed-forward modulation of the cortical state and a further investigation of the possible mechanism underlying the function of this modulation.

Chapter 5 demonstrates the faciliatory effect of CCK on LTP induction in cortical neurons and explores the possible mechanism underlying this effect.

Chapter 6 summarizes the findings and conclusions of the present study.

Chapter 2 Literature Review

A brief introduction of the auditory pathway is the first part of this literature review; this introduction emphasizes the effects of the MGB on the AC. Section two illustrates the functional application of parallel connections between the MGB and the AC.

Next, this chapter discusses neuronal plasticity. The third section briefly explores studies of learning and memory. The last section focuses on the topic of CCK, which is a key molecule in the present study.

2.1 Neuroanatomy of the mammalian auditory pathway

Compared to other modalities, auditory signals traverse more stages before reaching the cerebral cortex. In mammals, there are seven major components of the auditory pathway: the cochlea, the cochlea nucleus (CN), the superior olivary complex (SOC), the nucleus of the lateral leminiscus (LL), the inferior colliculus (IC), the medial geniculate body (MGB), and the auditory cortex (AC). This pathway is illustrated in **Figure 1**.

Sound waves are transformed into bioelectrical signals in the hair cells via mechanically gated ion channels. Due to the mechanical characteristics of the cochlea, hair cells exhibit frequency specificity. Hair cells in the cochlear base are tuned for high frequencies, and those in apex are tuned for low frequencies. Furthermore, ganglion cells of the cochlear nuclei make one-to-one connections with hair cells as has been shown in cats (Spoendlin 1972; Webster, Popper et al. 1992). In humans, some axons of the ganglion cells branch to form connections with two hair cells (Nadol 1983; Webster, Popper et al. 1992). Thus, the frequency information of particular sounds are specified in a tonotopic map, which is preserved in the ascending pathway.

The SOC lies in the ventral portion of mid-pons in humans. It receives most of

the synaptic input from the bilateral CN and sends its projections into the IC. The LL consists of ascending axons with several origins that include the CN and the SOC (Glendenning, Brunso-Bechtold et al. 1981; Webster, Popper et al. 1992). The IC is located in the dorsal horn of the brainstem, posterior to the superior colliculus (SC) (Rapisarda and Bacchelli 1977). It is the largest auditory center in the midbrain and consists of a large central nucleus and smaller surrounding nuclei that represent ascending and descending functions.

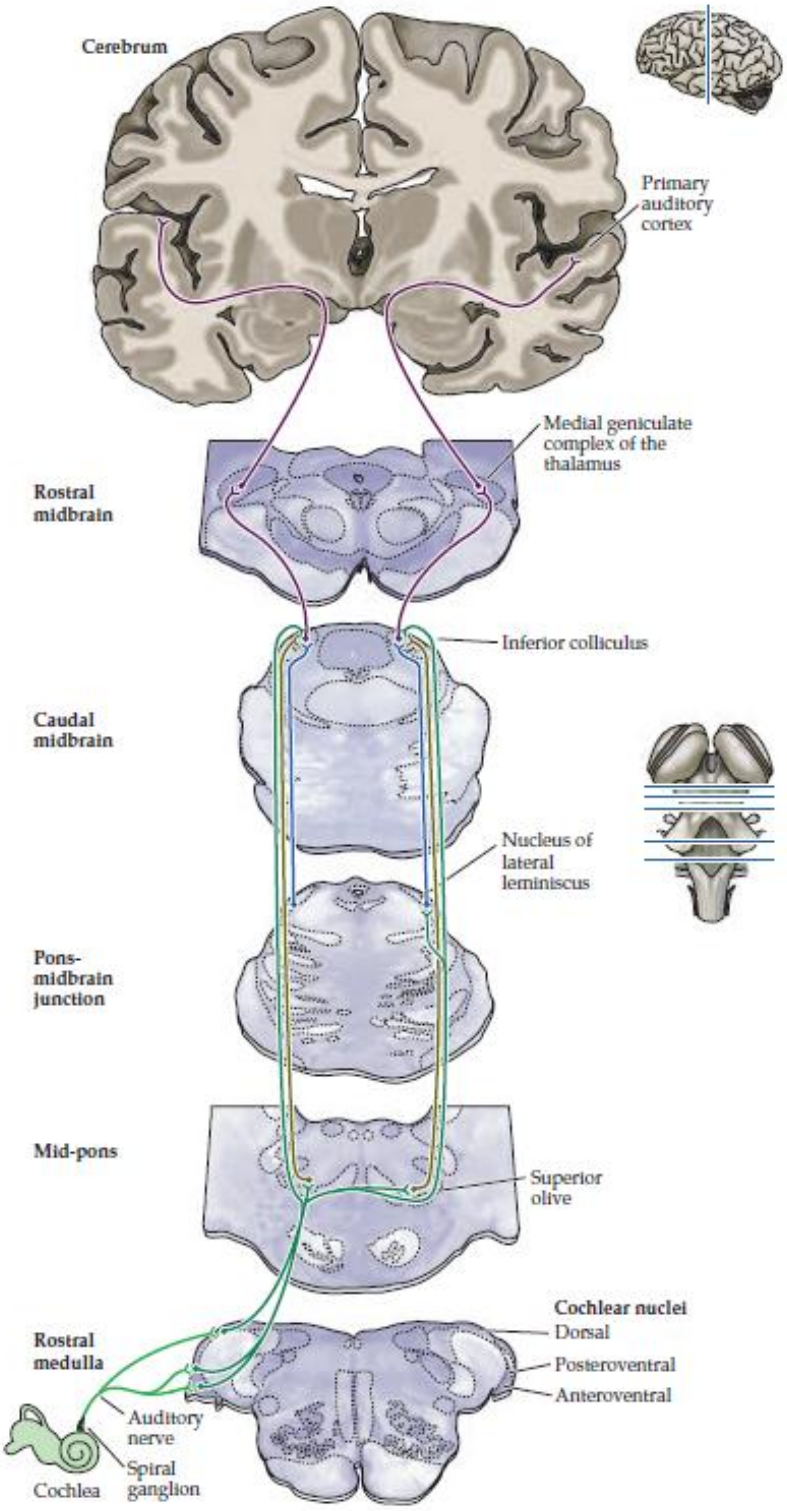

Figure 1 Diagram of the human auditory pathway (Purves 2004)

The MGB is the major auditory nucleus in the ventral thalamus. Another important auditory part of the thalamus is the auditory sector of the thalamic reticulate nucleus (TRN), which covers the lateral portion of the thalamus (Rapisarda and

Bacchelli 1977). The MGB is readily divided into the ventral (MGv), dorsal (MGd) and medial (MGm) (Winer, Miller et al. 2005). These divisions are distinguished by their different neuronal morphologies and cell densities, which can be shown with cytochrome oxidase staining (Anderson and Linden 2011) as shown in **Figure 2**. The overall organization of the MGB is similar across many species (Winer 1984; Winer 1985; Webster, Popper et al. 1992). The MGv is the largest portion and receives the greatest number of projections from the contralateral central nucleus of the IC. Dendrites of the neurons in the MGv are arranged in an orderly manner and, together with the regularly ordered cell bodies, form a laminar structure. Because of this, the MGv is regarded as a lemniscal portion of the MGB (He 2001). This laminar arrangement conserves and reflects the afferent inputs arising from the IC. Thus, the projection from the central nucleus of the IC to the MGv reiterates the frequency-specific pattern along the ascending auditory pathway. The neuronal architectures of the MGd and MGm are not as regular as that of the MGv. The ascending inputs to the former two nuclei are also different from those of the MGv. The MGd has diverse inputs that arise mainly from the brain stem. The origins of the projections to the MGm are even more diverse. These projections arise from the lower stages of the auditory pathway (IC, SOC, LL) (Kudo and Niimi 1980; Henkel 1983; Whitley and Henkel 1984)and some nuclei dedicated to other modalities (i.e., the SC and VN) (Graham 1977; Blum, Day et al. 1979) . The segregation of the projections into different divisions of the MGB indicates the distinct roles of these projections in auditory information processing.

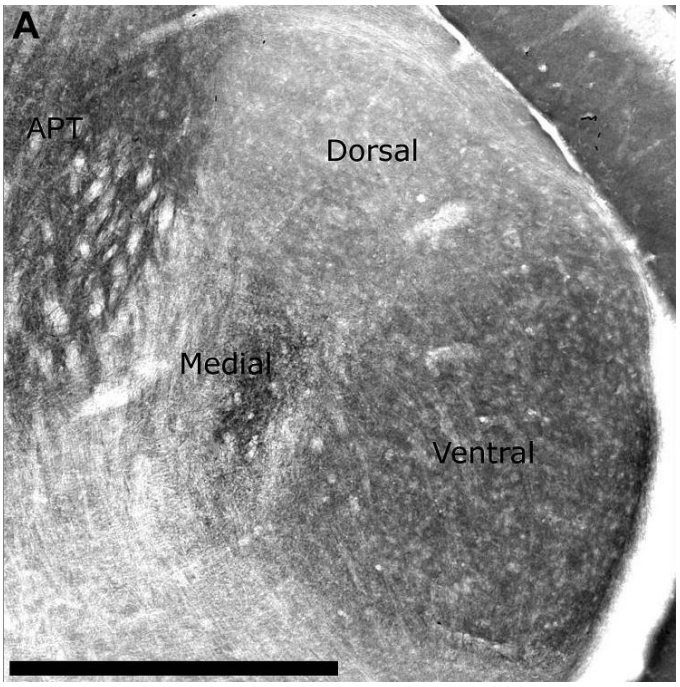

Figure 2 A coronal section through the MGB stained for cytochrome oxidase illustrates the histological identification of the auditory thalamic subdivisions; scale bar equals 1 mm; APT, anterior pretectal nucleus (Anderson and Linden 2011).

The AC is the auditory portion of the cerebral cortex. It is located in the temporal lobe of the cortex. Ascending projections originating from the MGB terminate in the auditory cortex. In the guinea pig, there are eight discriminable fields that are shown below in **Figure 3**.

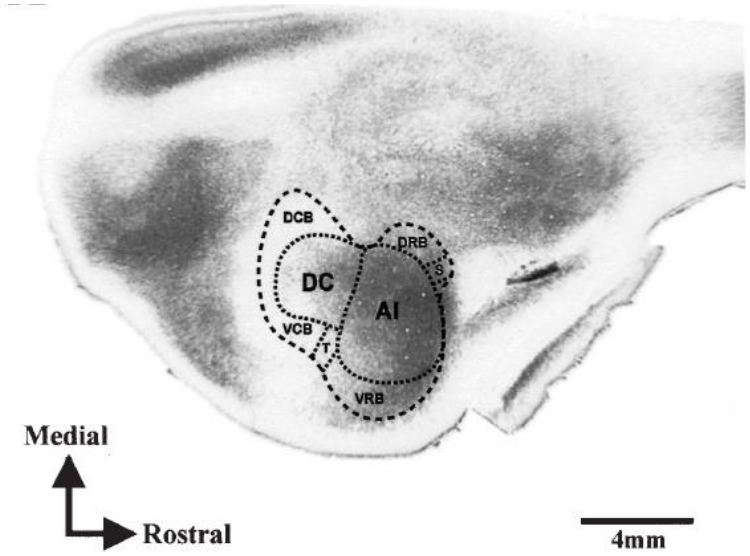

Figure 3 Auditory areas in the guinea pig cortex (Wallace, Rutkowski et al. 2000)

The primary auditory cortex (AI) is the largest of the auditory fields; it is defined by its distinct cytoarchitecture and connections with the MGB (Webster, Popper et al. 1992; Scannell, Burns et al. 1999). The characteristics of the AI include the following: short response latencies to acoustic stimuli, a smooth tonotopic gradient, a continuous frequency representation, and a thick granular structure (Wallace, Rutkowski et al. 2000). The non-primary auditory areas receive projections from the AI in addition to thalamic inputs. These non-primary areas have been suggested to be involved in the higher-order decoding of auditory stimuli rather than simple frequency-dependent responses (Popper and Fay 1992). For instance, experiments in cats have suggested the existence of orderly arrangements of unit clusters that respond to amplitude-modulated tones in contrast to the normal tonotopic map of the associated auditory field (Schreiner and Urbas 1988). Another topic of study has revealed that neural plasticity is also different between the AI and other areas. Experiments by Diamond and Weinberger show that, in the secondary auditory cortex (AII), nearly all neurons show plasticity during an associative conditioning task; this is in contrast to the 63% of neurons in the AI that show plasticity (Diamond and Weinberger 1984).

2.2 Structure and function of the parallel connections between the MGB and AC

The AC shares a laminar cytoarchitecture with much of the neocortex (Purves 2004). Layers with differences in cell numbers and densities can be shown histologically. In the AI, there are six layers that span from the outer surface to the white matter.

Layer I is sometimes called the molecular layer, as it mainly contains the axons and dendrites of cells located in deeper layers. Another prominent feature of layer I neurons is their lateral stretching dendrites. Their rich connections with apical dendrites from the pyramidal neurons of layer II to layer V have been suggested to have a broad and modest modulating effect in the cortex (Abeles and Goldstein 1970; Webster, Popper et al. 1992). Ascending projections to layer I have diverse origins

that are dominated by thalamic projection from the MGm (Mitani, Itoh et al. 1984; Winer 1984); this indicates a possible modulatory pathway from the MGm to the cortex via layer I. Layer II is rich in granule cells, hence it is called the external granular layer. Layer II mainly projects to the adjacent auditory field. It also provides interlaminar projections to adjacent layers. Layer III is called the external pyramidal layer and is a main source of commissural projections. Layer IIIb and Layer IV contain most of the terminals of thalamocortical projections. In contrast to the diverse origins of the projections to layer I, these projections are predominantly from the MGv (Steriade, Jones et al. 1997). These layers are sometimes termed receiver layers. The outputs of many layer IV neurons are to neurons in layers II and III, which pass ascending auditory signals insides cortex (Popper and Fay 1992; Thomson and Bannister 2003). Layer V is the internal pyramidal layer; it is the source of diverse connections that include corticocortical, commissural, corticothalamic (CT) (Webster, Popper et al. 1992; Scannell, Burns et al. 1999; Lee and Winer 2008) and corticocollicular projections (Schofield and Motts 2009).

Layer VI is called the multiform layer; it contains the most diverse neuronal populations of the AI. About half of layer VI neurons are estimated to project to the MGB, and they are the main source of corticofugal projections (Webster, Popper et al. 1992; Winer, Diehl et al. 2001).

In addition to layer specificity, thalamocortical (TC) projection also exhibit a distinct projection pattern that originates from different nuclei within the MGB. Extensive anatomical evidence supports the existence of segregated and parallel TC pathways that include lemniscal and nonlemniscal pathways (Jones 2001; Hu 2003). The lemniscal TC pathway passes on information from the ascending projections from the MGv that contain the main stream of auditory information. The non-lemniscal TC pathway arises from diverse origins and projects to broader cortical areas. In addition to the TC projections, the non-lemniscal portion of the MGB is also a major afferent source of inputs to the lateral amygdala, suggesting its role in emotional modulation (Weinberger 2011).

2.3 Learning, Memory and LTP

Memory is one of the most interesting topics in neuroscience. Memory refers to a process involving experience-dependent information encoding, storage and retrieval. Previously, the study of memory was the territory of physiology and later psychology. Many characteristics of memory have been described although the brain remains as a black box (Gentile and Miller 2009). In Pavlov's famous experiment, dogs successfully exhibited an artificial experience-dependent behavioral change that has been referred to as a type of memory. The conditioning-paired stimulation paradigms introduced by that experiment are still in use today with minor modifications. In spite of the fact that little is known about the physiological foundations, physiological and psychological studies provide us with some useful terms related to memory. For instance, we can discriminate memory into working memory, short-term memory and long-term memory; or we can discriminate different contents as explicit memory and implicit memory. Subsequent physiological studies have provided evidence suggesting that different types of memory systems exist in the brain and that memory formation relies on these different memory systems. These different memory systems are show in the following **Figure 4**.

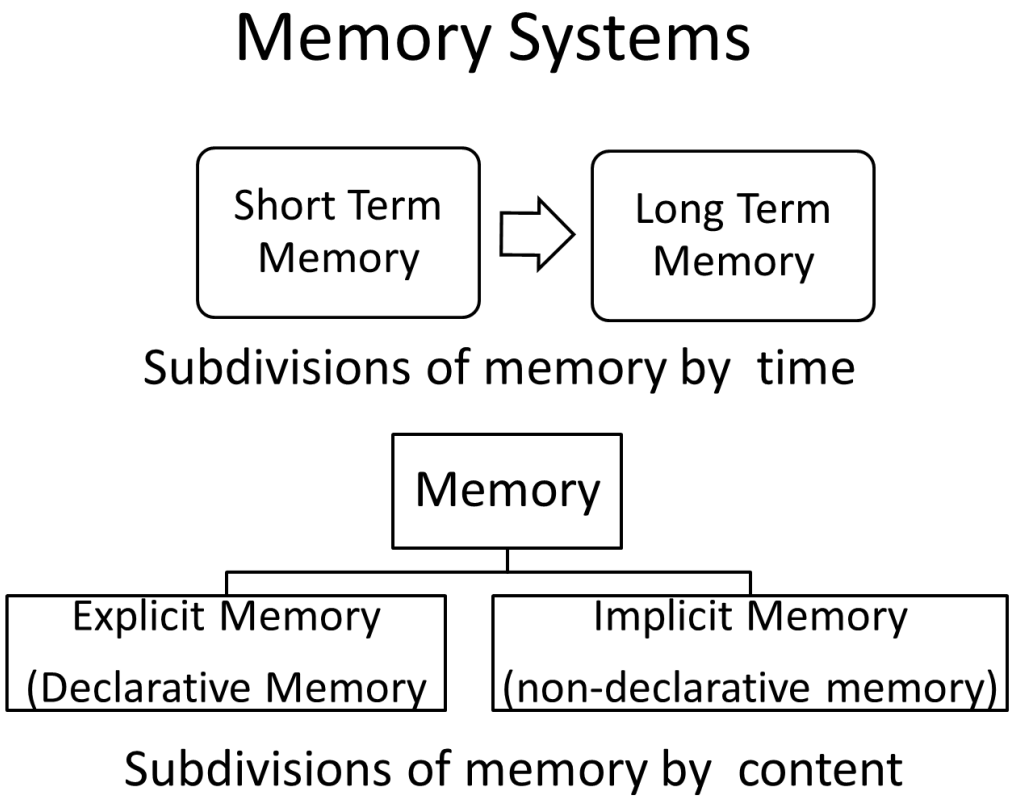

Figure 4 Different classifications of memory. According to its persistence through time, memory is subdivided into short-term memory and long-term memory; these forms of memory reflect the processing of acquired information in neural circuits in the form of spikes. Long-term memory depends on structural changes in the nervous system on molecular, cellular and circuit levels. Explicit and implicit memories are associated with different brain regions(Sweatt 2003).

Findings from, and subsequent studies of, the patient H.M. have been a crucial part of the history of the study of memory (Scoville and Milner 1957; Zola-Morgan, Squire et al. 1986; Krupa, Thompson et al. 1993). A prominent amnesia was found in H.M. after his bilateral medial temporal lobes (MTL) were surgically removed to cure his severe epilepsy (Scoville and Milner 1957). The ablated areas are shown in **Figure 5**.

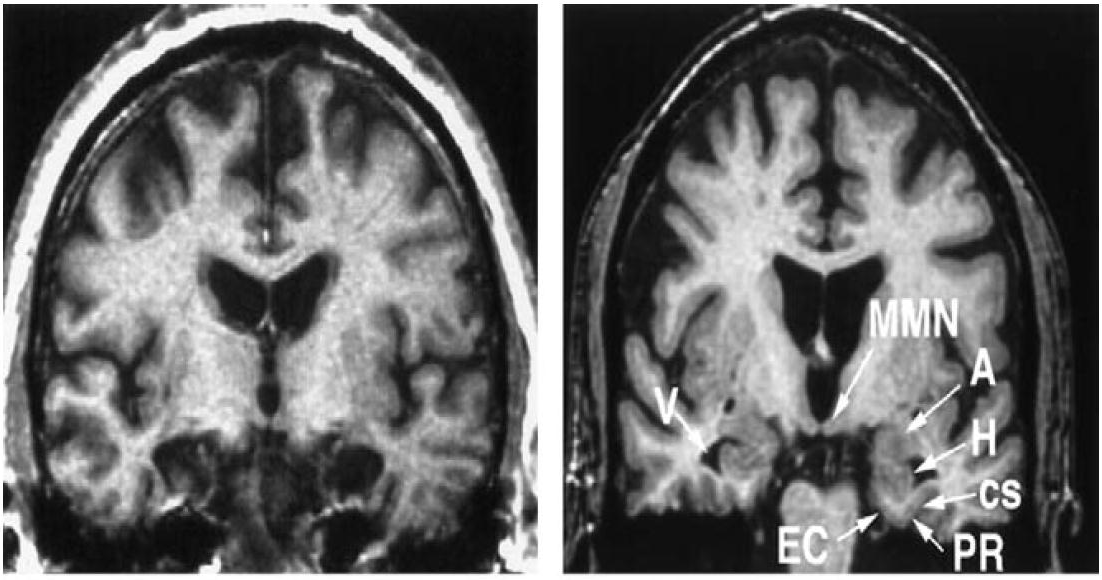

Figure 5 Magnetic resonance imaging scan showing the removal of the MTL in the patient H.M. compared to a control subject. The left is from H.M., the right is a scan from a normal control subject. The ablation included the entirety of the entorhinal cortex (EC), most of the perirhinal cortex (PR) of the amygdala(A), half of the hippocampus(H), which is shown in comparison with the control. CS, collateral sulcus; MMN, medial mammillary nucleus; V, ventricle. (Corkin, Amaral et al. 1997).

What we have learned from H.M. includes at least the following three key points:

1. The MTL is crucial for long-term memory formation. Ablation of the MTL in H.M. completely destroyed his capacity to form new long-term memories (Scoville and Milner 1957).

2. There are different memory systems in the brain. As shown in an experiment conducted on H.M., he was asked to practice drawing a five-pointed star shaped pattern over a period of several weeks. His performance in drawing improved gradually even though he could not remember practicing this task at all (Zola-Morgan and Squire 1993).

3. The MTL is not the ultimate storage point for long-term memory, especially permanent memories. As reported first in H.M., only recent memories were effected by lesions of the MTL, and remote memories were not affected (Scoville and Milner 1957).

Subsequent to the studies of H.M., more and more human cases of MTL lesions have been investigated, and animal models of amnesia have also been established (Squire, Amaral et al. 1989; Squire, Haist et al. 1989; Zola-Morgan, Squire et al. 1994). From those studies, the contributions of different parts of the MTL to memory have been discovered. A representation of MTL connectivity in the nervous system is shown in **Figure 6**.

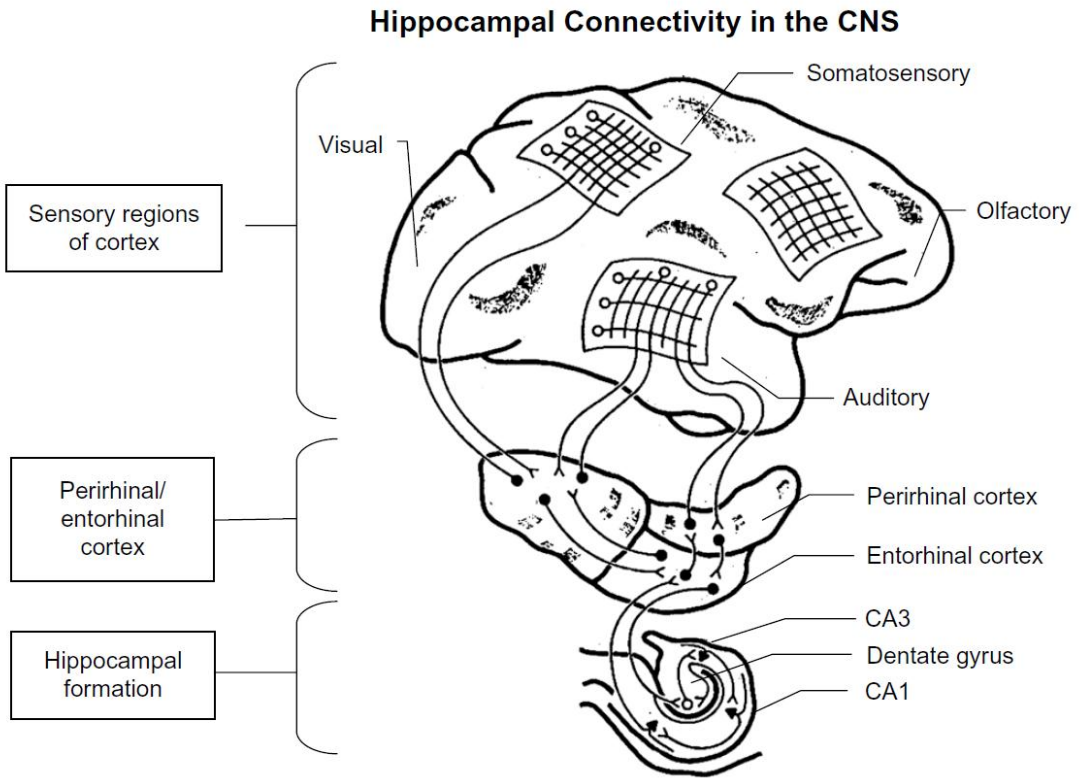

Figure 6 The hippocampal connectivity in the brain. Sensory signals are relayed to the perirhinal/entorhinal cortex between sensory cortices and the hippocampus. Figure from (Sweatt 2003)

Another branch of memory study focuses on the cellular mechanisms of memory. A famous statement was introduced by Hebb in 1949 (Hebb 1949); Hebb stated that neurons that fire together wire together. This postulate was later named as the Hebbian learning rule. This rule attempts to explain the cellular mechanism that underlies the behavior-associated learning that was shown in Pavlov's experiments. Direct experimental evidence supporting this theory was lacking for a long time until

the discovery of the LTP in 1973 (Bliss and Gardner-Medwin 1973; Bliss and Lomo 1973). As shown in **Figure 7**, repetitive pre-synaptic stimulation induced potentiation of the population EPSP, and stimuli with the same strength evoked larger responses after the induction process.

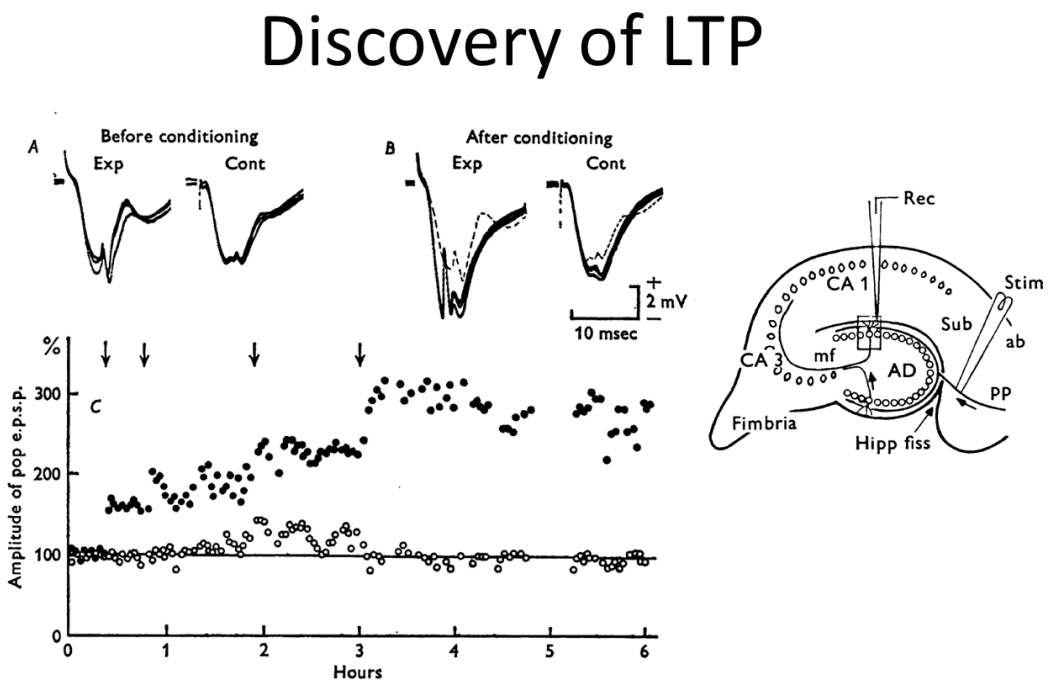

Figure 7 The first experiment to show LTP (Bliss and Lomo 1973). A conditioning stimulation made up of repetitive parings of pre-synaptic stimuli on the hipp fiss and post-synaptic action potentials that represented the population EPSP in CA1. The EPSP exhibited a long-lasting potentiation after treatment with the condition stimulation in experimental group (Exp, represented with filled dots)a. In the control group (Cont, represented with open dots), there was no conditioning. As result, no potentiation was observed in the control.

From then on, a growing number of experiments were conducted to explore the existence and properties of LTP. Additionally, long term depression (LTD)—a reverse form of LTP—was also discovered in 1982 (Ito and Kano 1982). In most experiments, LTP was found to be related to N-methyl D aspartate (NMDA) receptors, which are a subclass of glutamate receptors. A model based on NMDA receptors was established

to explain the cellular mechanism of LTP; and this model is illustrated in **Figure 8**. In this model, the NMDA receptor is a critical module, as it acts as a coincidence detector for pre- and post-synaptic activities. Pre-synaptic glutamate release and post-synaptic firing are essential to activate the NMDA receptor. Activation of the NMDA receptor opens calcium channels inside, which leads to an influx of calcium ions into the neurons and triggers downstream cellular signaling transduction. The extent of calcium elevation is also critical for plasticity, as shown by experiments with slowly repetitive stimuli or a reverse sequence of the pre- and post-synaptic activities that induces LTD instead of LTP (Bi and Poo 1998; Li, Lu et al. 2004). In an extent form of this model that is named spike timing dependent plasticity (STDP), back propagation of action potentials in the post-synaptic neurons determinates the timing by which LTP or LTD will be induced (Fuenzalida, Fernandez de Sevilla et al. 2010).

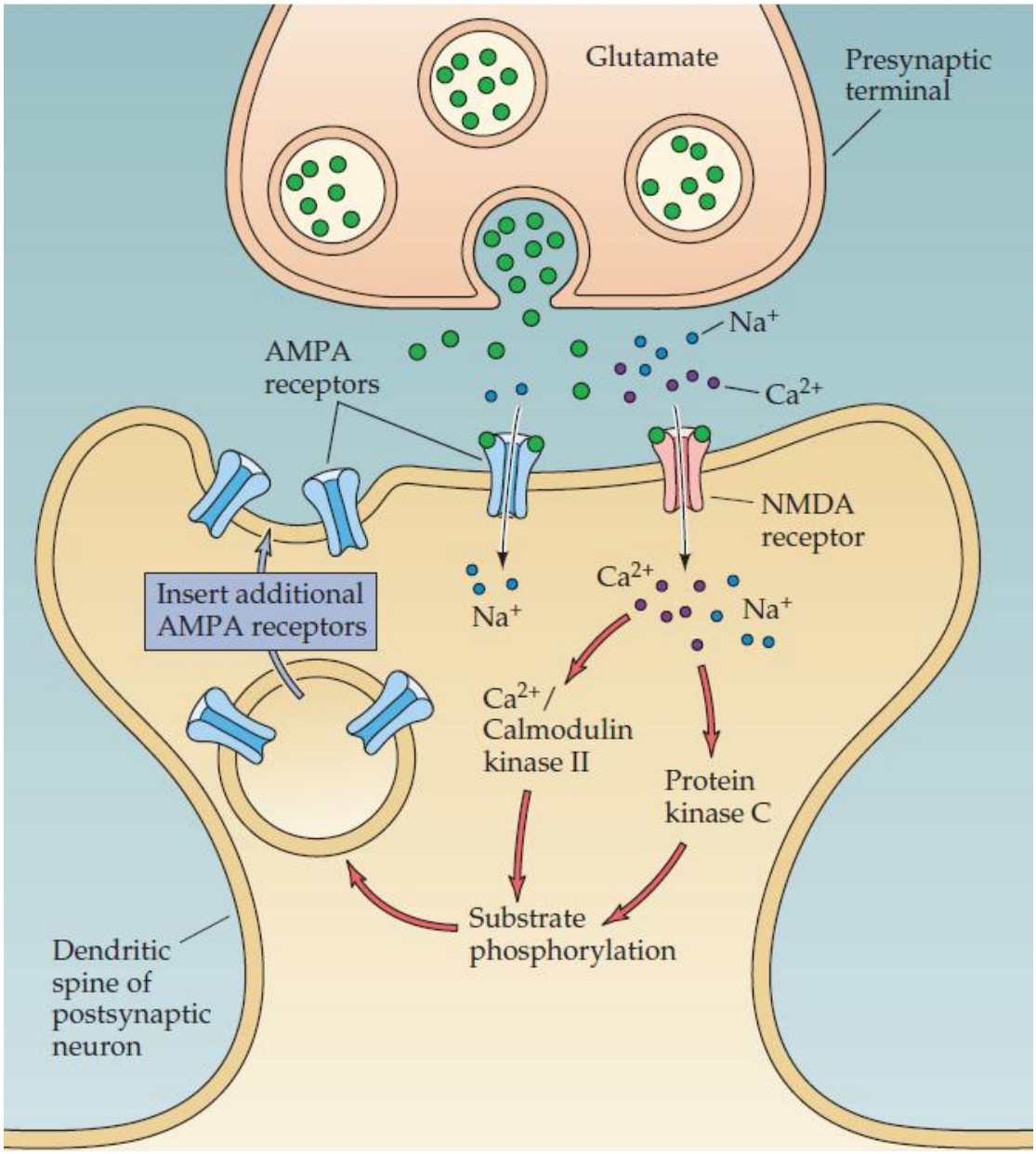

Figure 8 Mechanism of NMDA-dependent LTP. Glutamate released from the presynaptic terminal binds to AMPA and NMDA receptors in the dendritic spines of the postsynaptic neuron. During glutamate release, the NMDA channel opens only if the postsynaptic neuron is sufficiently depolarized. As NMDA channels are permeated by calcium ions during activation, the elevation of calcium activates subsequent signal transduction in the cell. As a result, more AMPA receptors are activated or inserted into the membrane of the cell. From (Purves 2004)

Increasing experimental evidence supports this NMDA-dependent model of LTP;

however, this model is not the only form of neural plasticity. There are other types of LTP that are NMDA independent. In addition, explanations of the timing between pre- and post-synaptic activities are still controversial. The cellular mechanisms of LTP are an ongoing hotspot in neuroscience. Although a full understanding of the mechanism of LTP is still far way, the application of LTP to the known neural structures has greatly extended our knowledge of the mechanisms of memory. For instance, a water maze study in rats has demonstrated the connection of LTP to spatial memory; in this study, the inactivation of hippocampal NMDA receptors resulted in the inability of animals to form spatial memories (Morris, Garrud et al. 1982).

2.4 CCK, properties and function

Cholecystokinin (CCK) was originally found in the gastrointestinal tract, where it acts in a manner similar to gastrin in that it results in the release of pancreatic enzymes, gall bladder contraction, and gastric motility (Beinfeld 1985; Lee and Soltesz 2011; Dockray 2012). CCK was later found to be present in the central nervous system (Vanderhaeghen, Signeau et al. 1975; Dockray 1976). The prominent form of CCK in neurons is a sulfate octapeptide (CCK-8S). CCK is first synthesized as a precursor of cholecystokinin that is then subjected to extensive tissue-specific posttranslational processing in spatially and temporarily selective manners. The processing of pre-CCK into CCK-8S is shown in **Figure 9**.

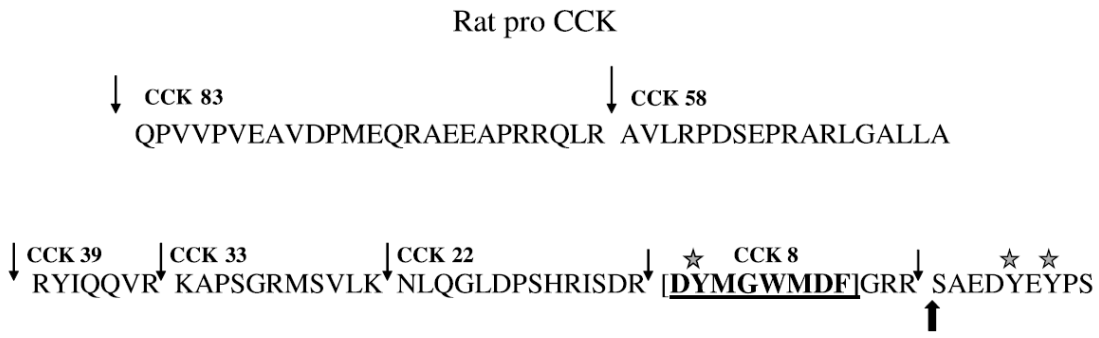

Figure 9 Synthesis and processing of neuronal CCK. The precursors are marked at their cleavage sites with vertical arrows. The string in bold represents the amino sequence of CCK-8S. The star marks the location of tyrosine sulfation sites (Beinfeld

2003).

CCK is one of the most abundant peptides in the nervous system, and it has a broad distribution across various brain regions; CCK has high levels of expression in the hippocampus, amygdala, cerebral cortex and olfactory bulb (Dockray 1976; Vanderhaeghen, Lotstra et al. 1980; Greenwood, Godar et al. 1981; Peters, Miller et al. 1983; Fallon and Seroogy 1984; Vigna, Morgan et al. 1984; Seroogy, Brecha et al. 1985). In addition to its wide distribution, another prominent property of CCK deserves attention: in the rat brain, its turnover is slower than that of other (Meek, Iadarola et al. 1983). As CCK shares a similar carboxy terminal structure , and other properties of gastric function, with gastrin, they have been suggested to have a common evolutionary precursor (Dockray 2012). When compared with CCK immunoreactivity, the distribution of CCK mRNA has a different pattern that is possibly due to alternate post-transcriptional processing. It is also due to the existence of CCK containing projections (Greenwood, Godar et al. 1981; Ingram, Krause et al. 1989; Lindefors, Brene et al. 1991). It should also be noted that CCK and other neural transmitters co-localize.

There are two types of CCK receptors that have been identified based on pharmacology. These receptors are named CCK receptor A (for alimentary, CCKAR) and CCK receptor B (for brain, CCKBR) (Dufresne, Seva et al. 2006). CCKAR is traditionally classified as a peripheral receptor that is mainly present in the gastrointestinal tract and also present in select central neural areas (Dufresne, Seva et al. 2006) .CCKBR is the prominent form of the CCK receptor in the central nervous system (Honda, Wada et al. 1993; Mercer, Beart et al. 1996; Desbois, Clerc et al. 1998). As has been shown in several radioligand binding studies, high concentrations of CCKBR are present in the cerebral cortex, the hippocampal region and the olfactory bulb (Honda, Wada et al. 1993).

The cellular mechanism of CCK has been investigated in several studies. It has been shown to act via calcium signaling neurons of the snail Helix aspersa through protein kinase C (Hammond, Paupardin-Tritsch et al. 1987). In another experiment

performed on cultured striatal neurons, CCK increased intracellular calcium concentrations through calcium channels (Miyoshi, Kito et al. 1991). A direct excitatory effect of CCK has been reported in rat spinal dorsal horn neurons (Willetts, Urban et al. 1985), rat dorsolateral periaqueductal gray neurons (Yang, Chung et al. 2006) hippocampal pyramidal neurons (Shinohara and Kawasaki 1997; Wang, Zhang et al. 2011), hippocampal interneurons (Miller, Hoffer et al. 1997), vagal afferent neurons (Zhao, Kinch et al. 2011) and cultured neurons from rat cerebral cortex (Delfs and Dichter 1985). The underlying cellular mechanism has been suggested to include activation of TRPC-like channels (Wang, Zhang et al. 2011; Zhao, Kinch et al. 2011), the suppression of post-synaptic leak potassium current (Miller, Hoffer et al. 1997), and a presynaptic action with an unknown mechanism (Delfs and Dichter 1985).

CCK has been reported to be involved in cognitive function in several previous studies. Intra-cerebroventricular administration of the CCKBR agonist pentagastrin impairs extinction of conditioned fear memory (Chhatwal, Gutman et al. 2009). CCK decreases exploratory tendencies in laboratory rodents after its injection(Crawley, Hays et al. 1981). It has also been shown that CCK prevents experimental amnesia in rats (Katsuura and Itoh 1986) and enhances the formation of memory retention in mice (Flood and Morley 1989).

Although the involvement of CCK in learning and memory and its downstream targets in cellular transduction have been noticed, explanations of the mechanisms by which CCK contributes to learning and memory are still an open question.

Chapter 3 Methodology

Part I In vivo experiments in guinea pigs

3.1.1 Acoustic Stimulation

Subjects were placed in a double-walled soundproof room (NAP, Clayton, Australia). Acoustic stimulation was generated with the auditory physiology workstation (Tucker Davis Technologies, USA). A close field speaker was connected to the ear bar, which was used to hold the skull of the subject. To facilitate sound conduction, a hollow ear bar was used. White noise with a frequency band of 10-30K Hz was used to evoke auditory responses. Sometimes, pure tones were also used to test frequency response characteristics as indicated.

3.1.2 In vivo experiment subject preparation

Healthy guinea pigs (*Cavia porcellus*) of both sexes, as shown in **Figure 10**, provided by central animal facilities (CAF), Hong Kong Polytechnic University, served as subjects for the in vivo experiments. Atropine sulphate in 0.9% saline (0.2 ml/kg, 20 mg/ml, Sigma) was administered via subcutaneous injection (s.c.) 10 min before anaesthesia to avoid tracheal obstruction. Nembutal (0.4 mg/kg, Abott, in the feed-forward thalamic modulation experiments, and neural plasticity experiments except the visual conditioning experiment) or Urethane (1.2 g/kg, 20% solution in 0.9% saline, Sigma, in the visual conditioning experiment) was used as anaesthesia via intraperitoneal injection. Supplemental injections of atropine sulphate and Nembutal or urethane were applied every 2 hours at 20% of the initial dosage. After anesthesia, a straight cut was made on the skin covering the trachea, and a half crosscut was made in the trachea to insert a Y-shaped tube. The subject was mounted in a stereotaxic instrument (SR-6R,Narishige). Artificial respiration was performed with a ventilator

(Harvard Instrument). The muscle relaxant gallamine triethiodide (50 mg/kg initially, 10 mg/kg/hr regularly, i.m.) was injected immediately after application of the artificial respiration. The anaesthesia was monitored through EcoG by an electrode placed on the surface of cortex. Occasionally, the chest of subject was opened, and the body was slightly hung up and the cerebrospinal fluid was released by piercing the dura mater through the foramen magnum to reduce vibration of the brain. The subjects' internal body temperatures were monitored with a probe inserted into the rectum and maintained with a heating blanket. A midline incision was made in the scalp, and craniotomies were created to gain access to the auditory cortex and MGB. The dura mater covering the auditory cortex was subsequently removed. All experimental protocols were approved by the Animal Subjects Ethics Sub-Committee of the Hong Kong Polytechnic University. License to conduct experiments using guinea pigs was issued by the Department of Health.

Figure 10 Guinea pig: model used for the in vivo experiments.

3.1.3 In vivo extracellular recording

Metal electrodes with impedances approximately 1 M ohms (FHC) were used to record extracellular spikes. Electrodes with impedances approximately 100 ohms were used to record local field potentials. A TDT pre-amplifier (RA16, TDT) was

linked to the electrodes, and a ground electrode was placed in the neck muscle. The ground was made of Ag/AgCl wire. The amplified signal was collected with a TDT base station RX5 and a digital converter Axon Digidata 1440A(Axon).

The recording sites in the cortex were based on the map of the auditory cortex of the guinea pig, as shown below. As there were many blood vessels on the surface of the cortex, recording electrodes were kept away from visible vessels. The configuration of the electrodes is shown in **Figure 11**

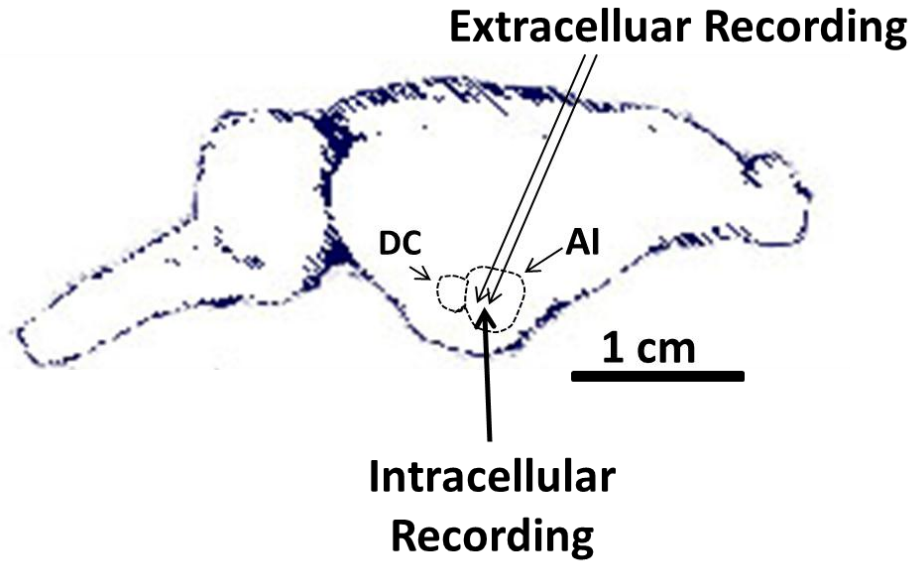

Figure 11 The configuration of the electrodes for the in vivo experiments. Extracellular electrodes and intracellular electrode were placed in the center of AI with distance around 2mm.

3.1.4 In vivo intracellular recordings

Intracellular recording of the primary auditory cortex was conducted. The locations referred to are the same as those used for extracellular recording. Blood vessels were also avoided to reduce damage and to increase the stability of intracellular recording. Intracellular electrodes were made from a borosilicate pipette filament (BF100-58-10, Sutter) using a Flaming Brown Micropipette Puller (P87, Sutter). 1 M potassium chloride or 3 M potassium acetate were used for pipette solutions; a tracer of 2% Neurobiotin (Vector) was added into the solution. The

impedance of the electrodes was between 50 and 90 Mohms. A step motor driving micromanipulator was utilized via the stereotaxic instrument. The electrode was held with the holder of the micromanipulator and advanced by the step driver. An Axon Amplifier 2B or 900A (Axon Instruments) was used to collect the membrane potentials （Vm）of the neurons. The impedances of the electrodes were also measured by the amplifier. Fast stepping was used to move the pipette tip close to the cortex. A rapid change in the Vm represented the contact of the electrode with brain tissue. Next, low melting temperature paraffin (42-45 ℃, Wako) was used to cover the exposure of the cortex to reduce vibration and create stable recordings. Four micrometer steps were used to search for neurons in the cortex. During recording, depolarization currents (0.5-2 nA) were injected through the electrode to evoke artificial action potentials.

The amplified intracellular Vm was also digitized through an Axon Digidata 1440 (Molecular Device, US) and stored in a computer with Axonscope (Molecular Device, US).

3.1.5 Electrical stimulation

In the primary auditory cortex, electrical stimulation was conducted with a train of high frequency pulses. The parameters were the following: 0.2 ms in width, 100 Hz frequency and 2 or 100 pulses per train depending on the experimental protocols. The parameters were based on previous work from the same lab (Xiong, Yu et al. 2004).

3.1.6 Labeling of intracellularly recorded neuron

After successful intracellular recordings, the tracer biocytin was injected into the neuron as needed through delivery of rectangular depolarization current pulses (3 Hz, 2 nA for 1-5 minutes). The subjects were kept alive for at least 30 min after tracer injection. When all the recordings were completed, the subjects were deeply anaesthetized with an overdose of Nembutal (2 ml/kg, 50 mg/ml, Abott) and perfused transcardially with 200 ml of warm saline solution (0.9% NaCl), followed with cold 4%

paraformaldehyde in 0.1 M phosphate buffer (pH 7.4). Subjects' brains were quickly removed from the skulls and infused in the 4% paraformaldehyde solution. After post-fixation for 4 hours, the brains were infused in 25% sucrose in phosphate buffer (0.1 M, pH 7.4) for 2 days at a temperature of 4℃. Coronal sections (with a thickness of 40 μm) of thalami and/or cortices were cut with a freezing microtome. Sections were collected in 0.01 M potassium phosphate-buffered saline (pH 7.4) and then incubated in 0.1% peroxidase-conjugated avidin-D (Vector) in potassium phosphate-buffered saline with 0.5% Triton X-100(Sigma) for 4-6 hours at room temperature. Sections were examined under a microscope to examine peroxidase activity with 3', 3'-diaminobenzidine (DAB). Sections containing labeled neurons were mounted on gelatin-coated slides and counterstained for Nissl substance.

3.1.7 Drug injection in the MGB and AI

Lidocaine was used for temporal inactivation of nuclei in the MGB. A glass pipette with a fine tip was filled with drug, and a metal electrode was combined with the pipette to monitor the effect of inactivation. In each section, 0.2 μl lidocaine was injected via a manual Hamilton Syringe(Hamilton, USA). Minimum volume of injection was adopted to block neural activities in a small area. The injection pipette was also placed in the center of MGm or MGv.

The location of the MGB was based on an atlas of the guinea pig's brain (Rapisarda and Bacchelli 1977) and previous works of our lab (He 1997; He 2001). After physiological recording, the location of the injection was labeled with electrical lesions using the metal electrode. One milliamp direct current was applied for 15 s to create lesions that could be shown with Nissl staining. The experimental configuration is shown in **Figure 12**

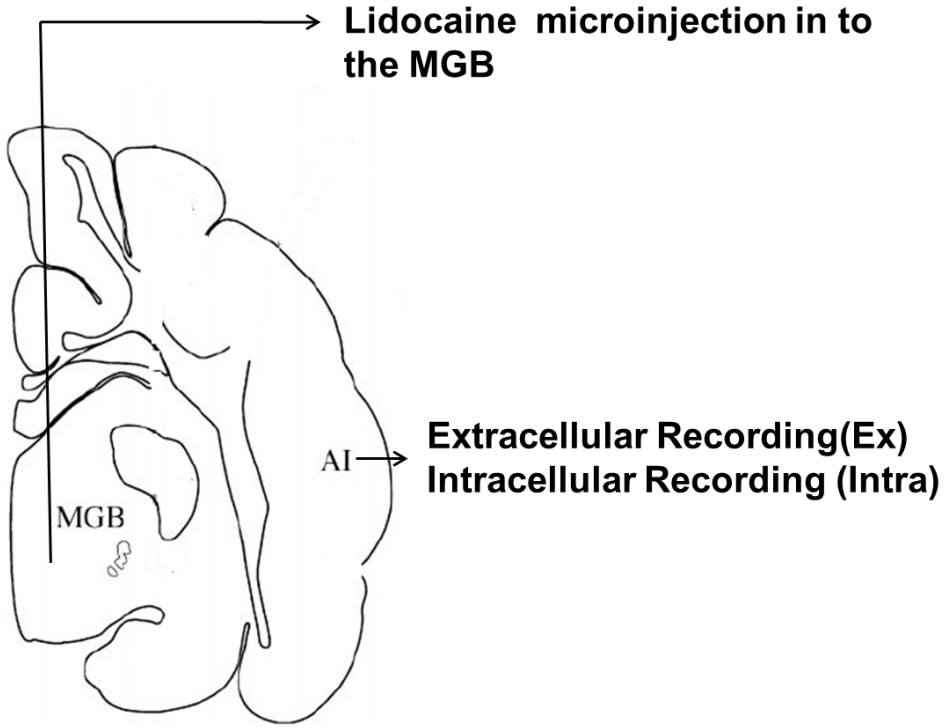

Figure 12 Schematic diagram of the experimental configuration for MGm inactivation

Study of neural plasticity in the AC. Local application of CCK was conducted via the same protocol used to inactivate the MGB. The configuration of all electrodes is shown in **Figure 13**.

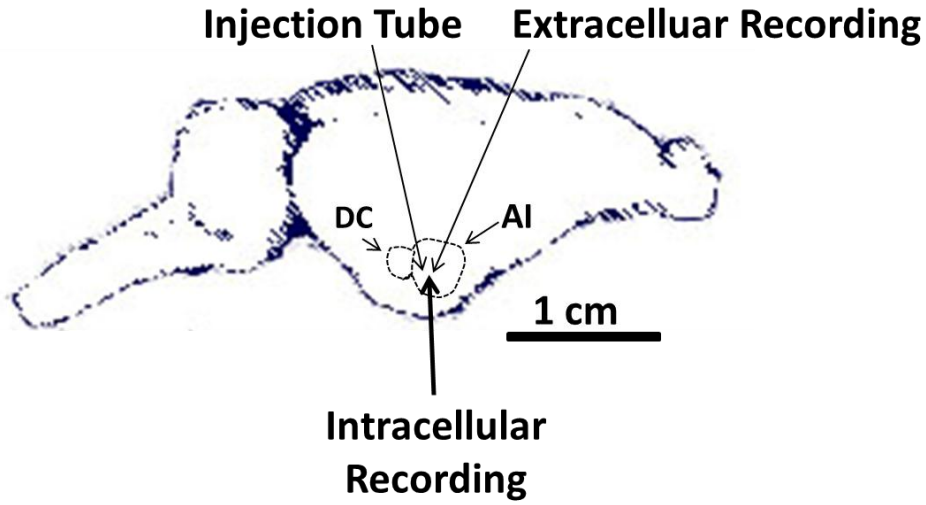

Figure 13 Electrode configuration for the in vivo LTP experiment

Part II In vitro experiments in dissociated cortical neurons

3.2.1 Isolated cortical neuron culture

Primary cultured cerebral cortical neurons were obtained from 18-days-old Sprague Dawley rat embryos with methods similar to those described previously(Bi and Poo 1998). Briefly, the neocortex was dissected and incubated with 0.25% trypsin at 37 ℃ for 15 min. Cells were then mechanically dissociated using a Pasteur pipette with a fire-narrowed tip in the culture medium and plated at a low density of 1000 cells/ml on 35-mm culture dishes pre-coated with poly-L-lysine (10 μg/ml). Cells were maintained in neurobasal/FBS medium containing 0.5 mm glutamine, 100 units/ml penicillin, and 100 μg/ml streptomycin under a humidified atmosphere of 5% CO2, 95% air at 37 ℃ for the first 24 hours and then changed to another medium in which FBS was replaced with 5% B27 supplement. Half-changes of medium were performed twice weekly. Cells were used for electrophysiological recording at 8–21 days after plating.

3.2.2 Whole cell patch clamp recording

Patch clamp recording was conducted on the cultured pyramidal neurons that were aged between 8-21 days. An inverted microscope(Nikon, Japan) was used to visualize the cell culture dish. Pipettes were driven with three-axis hydraulic micromanipulators (Narishige, Japan). The Vm of the neurons was continuously recorded. Signals were amplified with a Multiclamp 700B amplifier, digitized with a Digidata 1440 and acquired with pClamp 10 software (Molecular Device,USA). The bath solution contained (in mM) 145 NaCl, 3 KCl, 2 MgCl2, 3 CaCl2,10 HEPES, 10 glucose, pH 7.4 with NaOH, 300 osmol/L. Patch pipettes with resistances between 3-8 MΩ were pulled from borosilicate glass (WPI, USA) with a Sutter-87 puller (Sutter, USA). Pipettes were filled with a solution for voltage clamp recording that contained (in mM): 145 K-gluconate, 0.2 EGTA, 10 HEPES, 5 NaCl, 1 MgCl2, 4 Mg-ATP, and 0.3

Na-GTP, pH 7.2 with KOH, 285 osmol/L. To avoid dialysis of the cellular components, amphotericin B (Sigma, 200 ng/ml) was added to the internal solutions to create perforated recordings. The series resistances were about 30 MΩ and were stable throughout recording; data were discarded if series resistances changed excessively.

3.2.3 Drug puffing system

Glutamate-puffing was used to activate the recorded neurons directly. Fifty micromolar glutamate was locally applied for 20-100 ms with a pressure of 10 psi(pound per square inch) compressed nitrogen controlled by a Picospritzer III (Parker, USA). Cholecystokinin (CCK-8s, 2 μM, Tocris) was delivered via another glass pipette, and two pipettes were positioned in parallel to activate the same soma or dendrite areas. External solution was perfused nearby to wash out residual puffed drugs with a homemade continuous perfusion system. The duration of glutamate puffing was adjusted to evoke small EPSPs. The duration and timing of application of both drugs were controlled digitally with the Clampex10.0 (Molecular device, USA). The configuration of puffing tubes and recording electrode is shown in **Figure 14**.

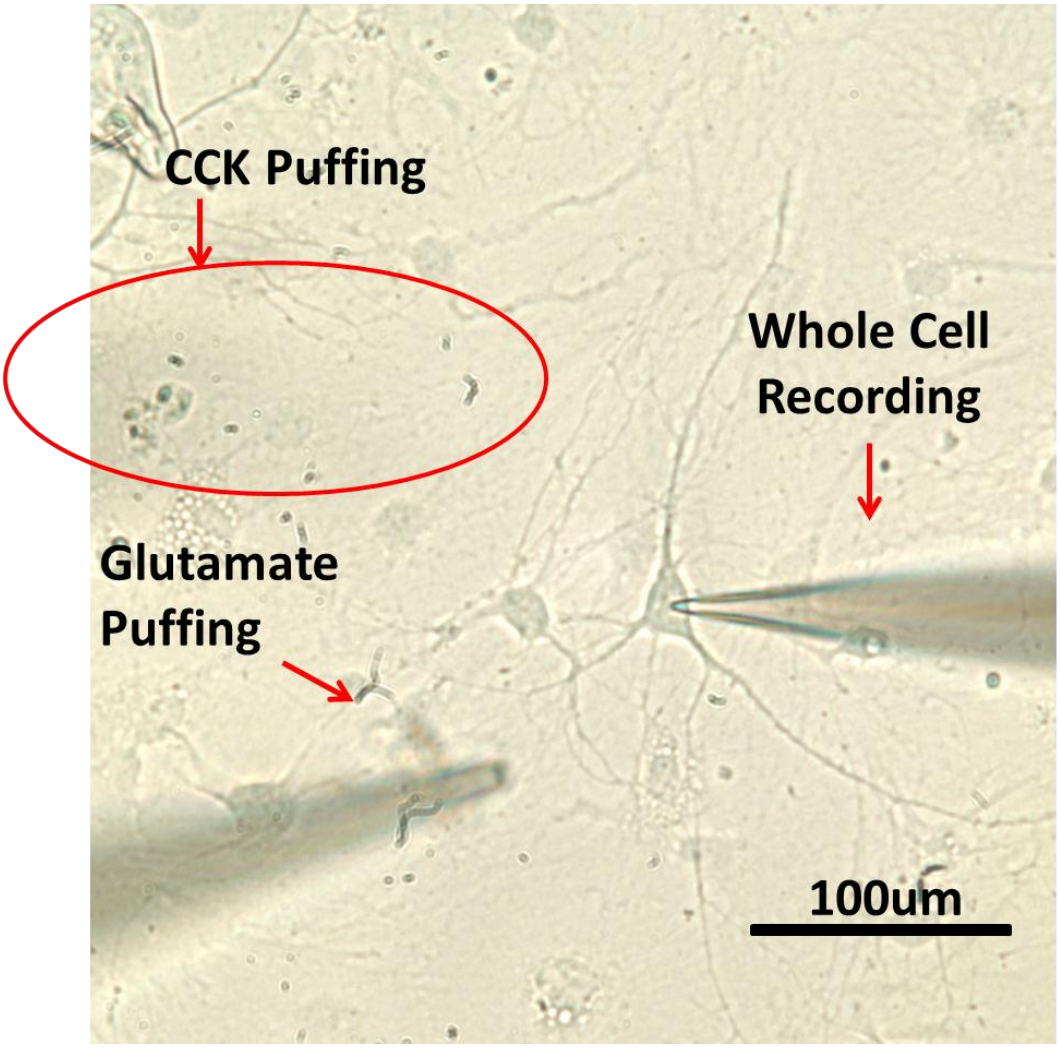

Figure 14 Experimental configuration for the in vitro experiments. Whole cell recording was conducted by a glass pipette on the right. On the left side, two glass pipettes were used to deliver glutamate and CCK respectively. The CCK pipette was moved close to the recorded neuron only when the conditioning was conducted, so that it was shown as shadow in the elliptical region.

Part III Experimental protocols and data analysis methods

3.3.1 In vivo Intracellular recording

Intracellular recordings from the MGm inactivation experiments were used for the analysis of evoked EPSP onset latencies. The time of injection was taken as a demarcation point, recording just before that time is referred to as pre-group, and recordings 5 min after the injection time are referred to as post-group. The measurements of latencies were based on 50 repeats. Paired t-tests were conducted on the group data from all neurons that were successfully recorded while the MGm was inactivated.

In the study of neural plasticity using an in vivo intracellular approach, the continuous recording of the Vm of neurons allowed us to measure evoked EPSP amplitudes. To minimize bias caused by spontaneous shifts in Vm, 10 repeats of the Vm recordings were averaged for measuring. The experimental flow chart is shown in **Figure 15**.

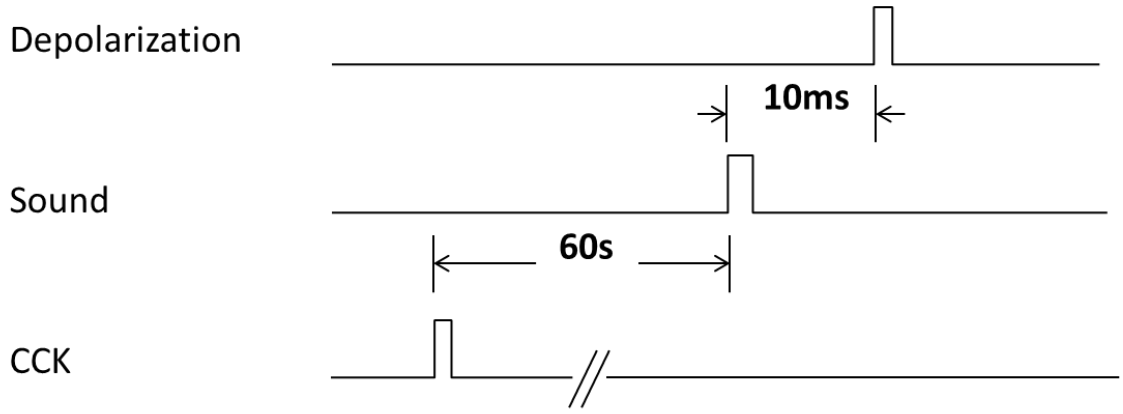

Figure 15 Schematic diagram showing the timeline of the LTP induction process for the in vivo experiment.

3.3.2 Extracellular spikes counting

The extracellular signals were stored with Brainware software（TDT, USA）. Raster plots of the spikes were used to show the firing rates and firing patterns in

response to acoustic stimuli. The timestamp of each spike was isolated from the raw data in the Brainware (TDT, USA) format. The first spike latency was defined as the time between the onset time of acoustic stimulation and the first spike after the stimulation in a 50 ms time window. Sweeps with no spikes in that time window were excluded from counting. All samples in which the MGm was inactivated were summarized, and the first spike latencies are shown in a post stimulation time histogram. The firing rate of each neuron was calculated as the number of spikes in the 50 ms time window divided by the sweep number. A paired t-test was conducted on the samples in which the MGm was inactivated.

3.3.3 Experimental protocol and data analysis methods for in vitro whole cell recording

The in vitro experimental protocol is shown in **Figure 16**. Puffing of glutamate was used to mimic pre-synaptic activity, and the action potentials evoked by depolarizing currents are referred to as post-synaptic activity. The puffing of CCK was a third factor in the present protocol.

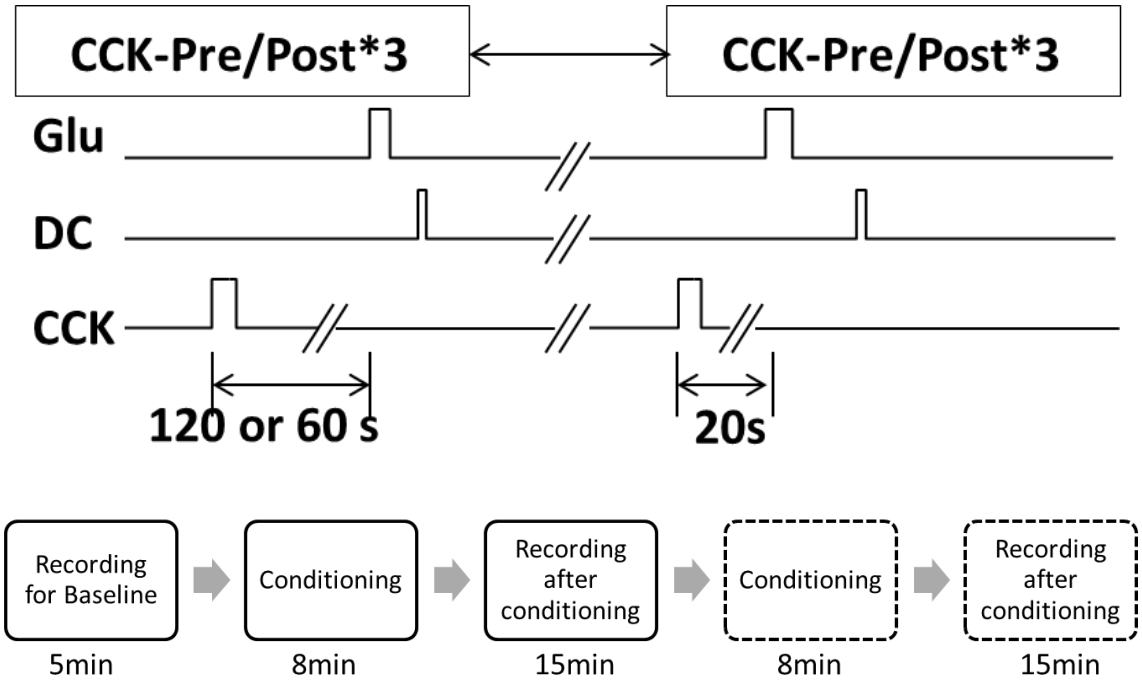

Figure 16 Schematic flow chart of the in vitro experiments on cultured neurons. The

intervals of between CCK and glutamate puffing were subject to change. Depending on the experimental design, 120 s or 60 s intervals were used. The conditioning stimuli were repeated three times for each interval. After the first section of LTP induction, a second one with a 20 s interval between CCK and glutamate was conducted if the recordings were stable for a sufficient amount of time.

Conditioning was produced by pairing the simultaneous puffing of glutamate and CCK with a depolarization of the recorded neuron that triggered an action potential (200 ms), as shown in Figure 17. Off-line data analyses were performed with Clampfit10.2 (Molecular Device, USA). The processed data were imported into SigmaPlot (Systat, USA) to generate graphs.

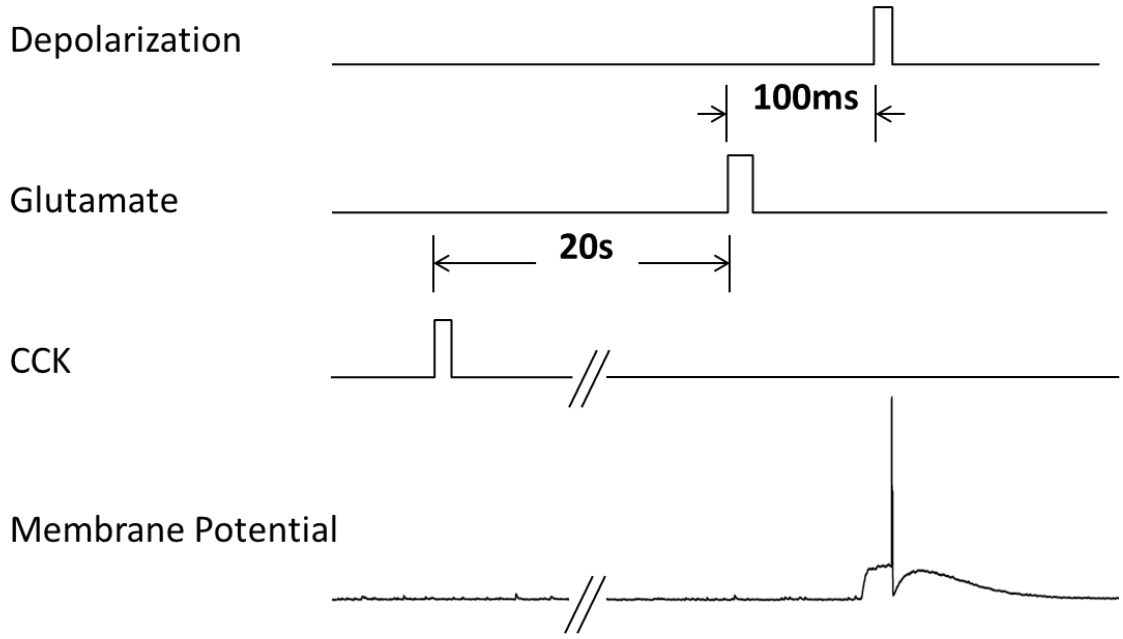

Figure 17 Schematic diagram showing the timeline of LTP induction by conditioned pairing in the in vitro experiment. CCK was puffed 20 s before the conditioning stimulation. An appropriate amount of glutamate was puffed to evoke EPSPs but not action potentials in the recorded neuron. A depolarizing current was injected 100 ms later within the EPSP process.

Chapter 4 Feed-forward thalamic modulation of the auditory cortex

The paralleled thalamocortical projections from different nuclei in the MGB have been identified as leminiscal and non-lemniscal parts. The leminiscal one origining from MGv constitutes the main part of thalamocortical projections and has a regular arrangement of cell bodies and fibers. It is supposed to be driver passing auditory information from thalamus to the cortex. However, functions of non-lemniscal part are still unclear. Based on its diverse projection pattern and short auditory response latency, we hypothesized that the non-lemniscal MGm has a feed-forward modulation to the neuronal response in the cortex, to the later coming signals from the MGv. In this part of the study, we investigated the feed-forward thalamic modulation of the auditory cortex in anaesthetized guinea pigs. There were 38 guinea pigs in this part of the study. First, we recorded the normal neuronal activities of cortical neurons in an anaesthetized condition. Both intracellular and extracellular electrodes were placed in the AC.

4.1 Normal Neuronal Activities in the AC of Anaesthetized Guinea Pigs

As shown in **Figure 18,** there was one channel for the intracellular electrode and four channels for the extracellular electrodes. We also placed a metal electrode in the MGB to monitor activity and to examine the validity of MGB inactivation. Four channels of extracellular and intracellular recordings exhibited synchronized responses to sound stimuli. Recordings in the MGB also showed corresponding responses that indicated an active status of the MGB.

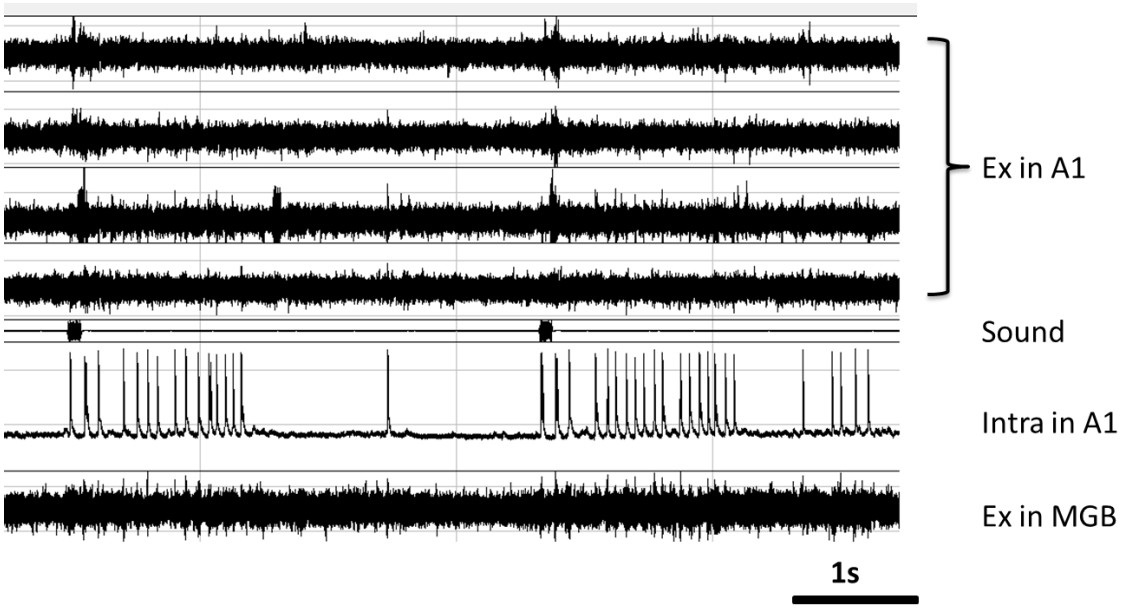

Figure 18 Simultaneous recordings in the cortex and the MGB. The upper four panels represent 4 extracellular channel recordings from the cortex via a vertical multiple electrode array. The distance between two electrodes was 250 μm. "Sound" indicates the onset of an acoustic stimulus of Gaussian noise. A train of spikes were present in the intracellular recording. Extracellular recordings in the MGB were taken via a metal electrode combined with the injection tube, and the activities of the neurons was shown be responsive to sound before drug injection.

4.2 Inactivation of the MGB by Local Administration of Lidocaine

The MGm has been hypothesized to modulate the state of the auditory cortex. We tried to temporally inactivate the MGm through local administration of lidocaine. Lidocaine is a sodium channel blocker that prevents action potential formation and propagation. As the thalamus is thought of as a main relay station for auditory information travelling to the cortex, the inactivation of the auditory portion of the thalamus should affect auditory responses in the auditory cortex. In **Figure 19,** the progress of MGm inactivation is presented. Continuous intracellular and extracellular recordings in the AC were performed. Lidocaine injection in the MGm abolished the neuronal activity around the injection site, as shown in the extracellular recordings in the MGB.

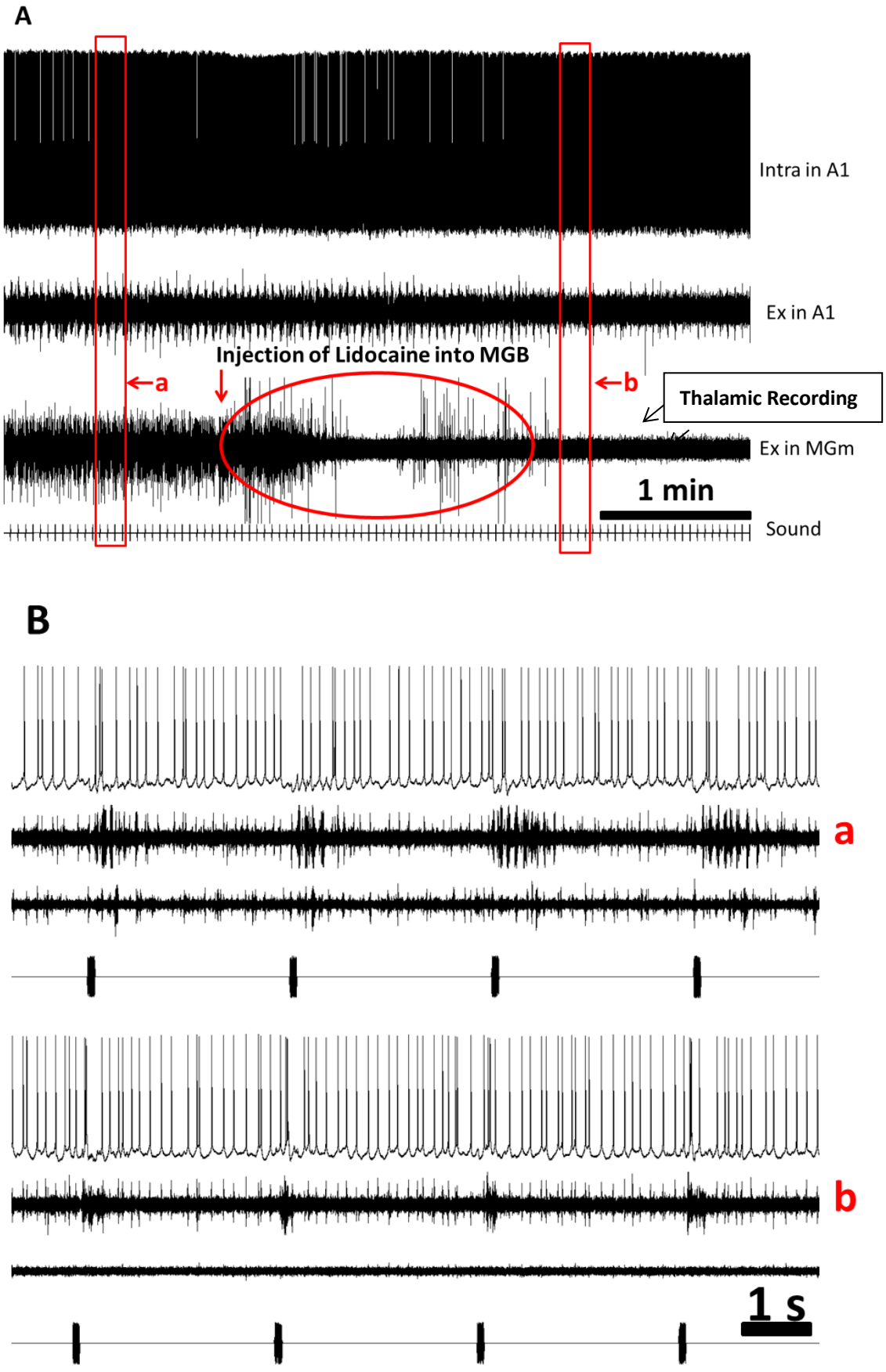

Figure 19 Progression of MGB inactivation. A, lidocaine was injected into the

MGm at the time indicated by the arrow. Extracellular recordings from an electrode combined with the injection pipette demonstrate the inactivation of the MGm. B, Recordings in the red boxes are shown on a magnified time scale. Responses to the sound are present in both the intracellular and extracellular recordings. Extracellular recordings in the MGm show that auditory responses were abolished after injection of lidocaine.

4.3 Inactivation of the MGm changed the auditory responses of cortical neurons

The extracellular activities of cortical neurons were collected through extracellular electrodes implanted in the auditory cortex. As described above, the MGm was temporally inactivated. The auditory responses of the AC exhibited obvious changes as shown in the raster plots of extracellular spikes (**Figure 20**). In the same preparation, repeated injections produced similar effect to the first injection. The reproducible changes also confirmed that the inactivation of the MGm was reversible. Before the inactivation, auditory responses exhibited a clean onset edge and subsequent oscillatory activities. After the injection, the onset responses were not well-ordered and the oscillatory activities were not locked to the acoustic stimuli.

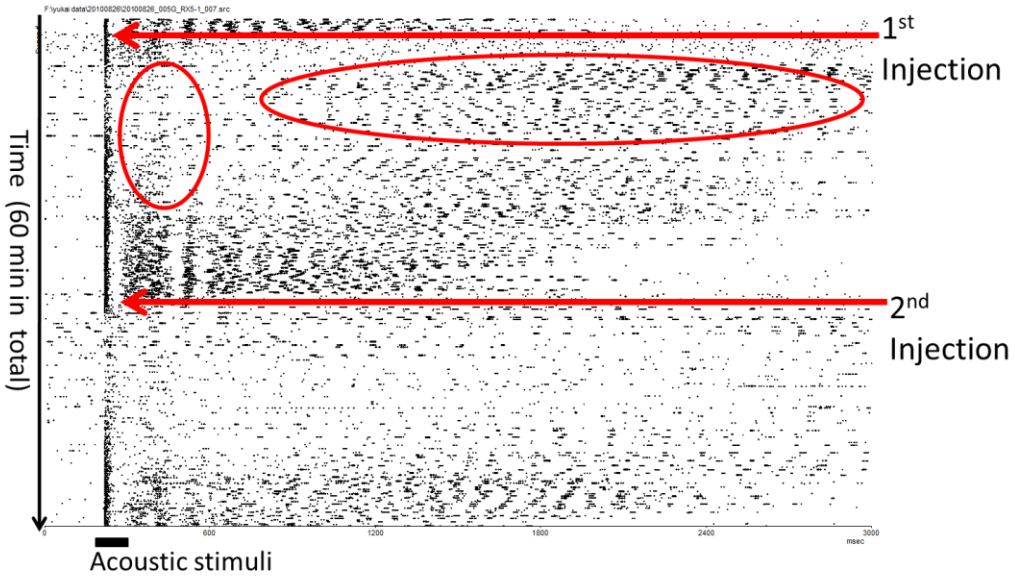

Figure 20 Reversible inactivation of the MGm changed the response pattern of

cortical neurons to sound stimuli. A raster plot shows 600 traces of extracellular recordings of spikes in the auditory cortex, each trace represents a trial of responses to a single stimulation, and each spot represents a spike. The time axis represents the sequence of recordings. In this case, 2 lidocaine injections were applied at different times as indicated in the figure. Initially, sound evoked responses consistent with the onset of firing and subsequent oscillatory firings, which are shown in the first several rows of the raster plot. The first injection disturbed the onset and the oscillatory firing pattern; only the onset firing persisted. However, as marked with the horizontal ellipse in the figure, there was spontaneous oscillatory firing. The second injection produced a similar effect as the first injection, indicating that the inactivation of the MGm and its corresponding effects were reversible.

To further analyze the changes, we made post stimulus time histograms of the spikes in a 500 ms time window starting 100 ms prior to the stimulus (**Figure 21**). Spike counts in which the MGm was intact exhibited a sharp peak at 18 ms, which represents the first spike latencies, and subsequent small peaks at 200 and 400 ms that correspond to the oscillatory activities in the raster plot (**Figure 21B** upper). However, spike counts in which the MGm was inactivated showed only a small and obtuse peak that had a delayed latency (**Figure 21B**, lower).

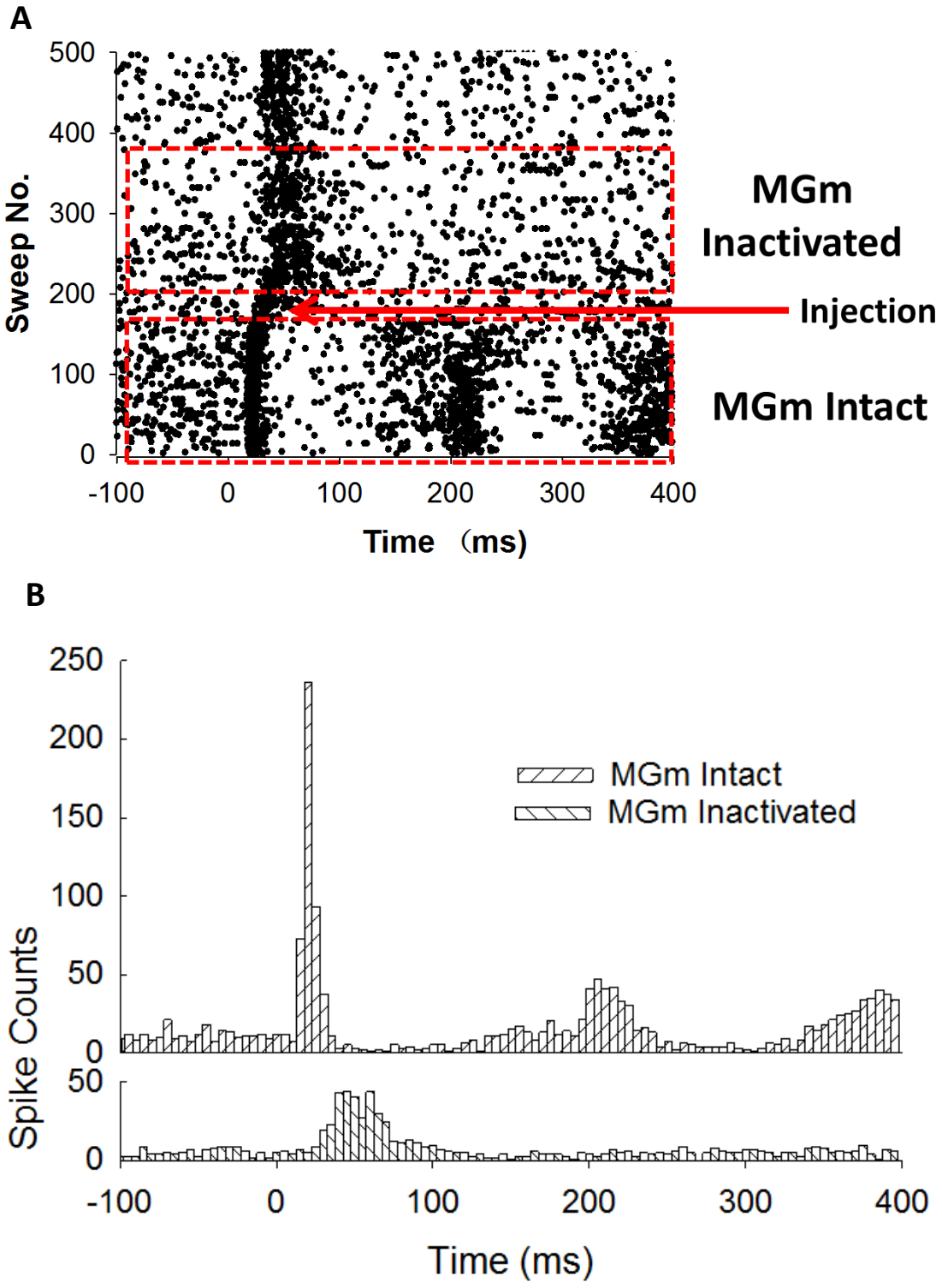

Figure 21 Inactivation of the MGm postponed the acoustic responses of cortical neurons.

A, Raster plot showing the spikes of a single channel extracellular recording. Vertically aligned dots visualize the onset of responses to the acoustic stimuli. The sweep no from 0 to 500 indicate the sequence of recordings. Lidocaine injection

prolonged the latencies of the responses.

B, Plots in the dotted boxes from Figure 21A converted to histograms. Cumulative distributions of spike latencies are presented. A sharp peak in spike latencies was present when the MGm was intact, and inactivation of the MGm caused a shift in the distribution as shown in the lower panel. Furthermore, the subsequent oscillatory responses following the onset responses in each trial as shown in the second and third peaks in the upper panel disappeared after inactivation of the MGm.

Next, we combined 488 extracellular recordings in which the MGm was inactivated. These recordings were obtained from 28 individual guinea pigs. With the injection time as a dividing point, all recordings were divided into two groups: MGm Intact and MGm Inactivated. Because the inactivation of the MGm was temporary, only the first 50 trials in each group were included in further analyses. The latencies of the first spikes in the first 50 ms time window after the onset of acoustic stimuli were extracted and plotted in PSTHs segregated by the two groups (**Figure 22A**). In contrast to the sharp peak observed in the MGm Intact group, the spike counts of the MGm Inactivated group exhibited a mild peak. Moreover, the overall spike count for the MGm Inactivated group was less than that for the MGm Intact group, which indicates a decrement in the spikes in response to the onset of sound stimuli when the MGm was inactivated. When comparing the means of the first spike latencies between the two groups, we found that the onset of the responses were delayed by inactivation of the MGm (**Figure 22B**).

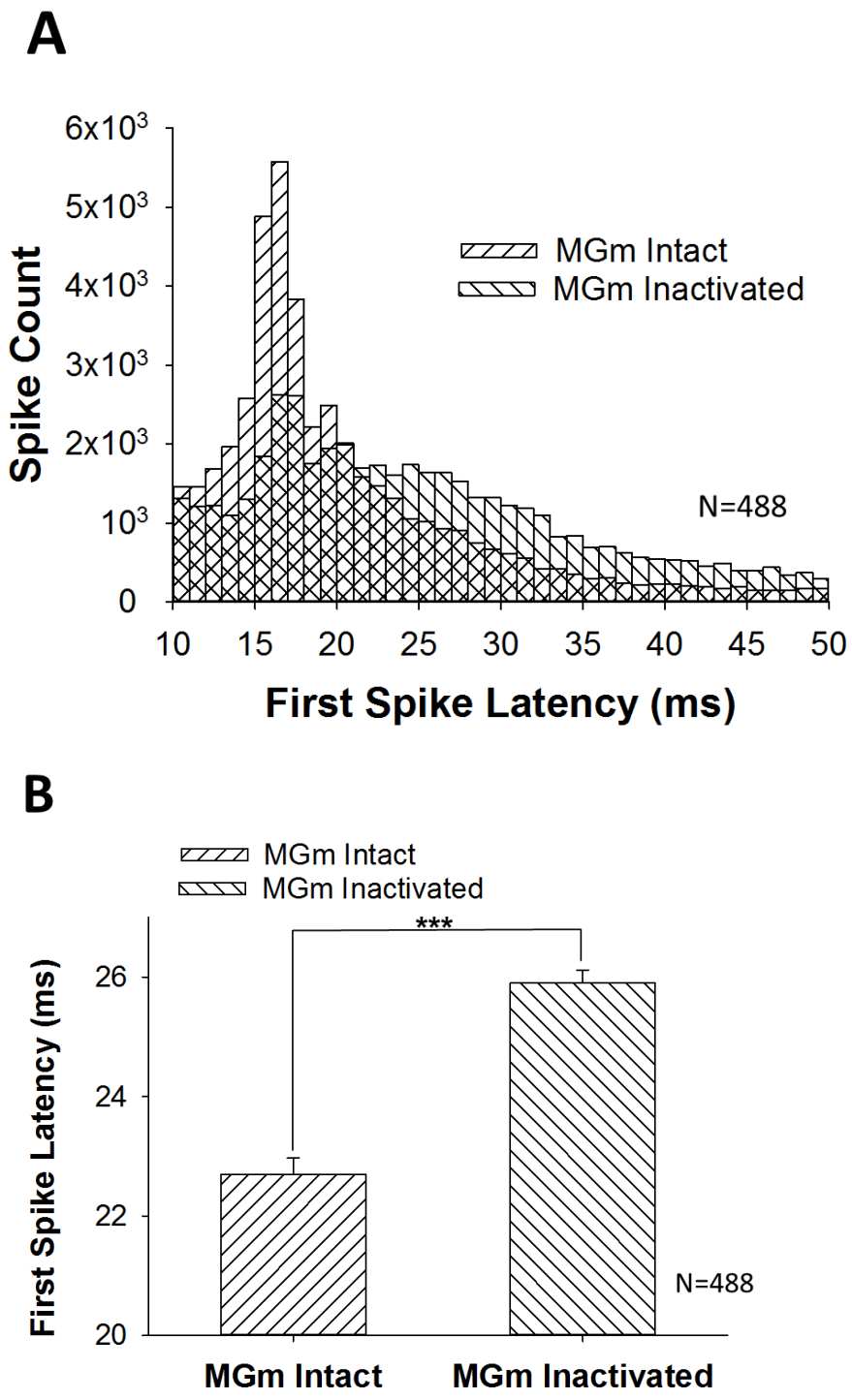

Figure 22 Summary of the changes in first spike latencies in the extracellular recordings. Here, the results from 488 units are summarized. The first spike latency was defined as the time from the onset of acoustic stimulation to the first spike within a 50 ms time window in each sweep; sweeps without any spikes in this period were excluded.

A, Histogram displaying the overall distributions of first spike latencies when the MGm was intact and inactivated. The peak of latency when the MGm was intact was 16 ms, but this peak was not prominent when the MGm was inactivated.

B, Means and standard errors of the first spike latencies when the MGm was intact and when it was inactivated. Statistical analysis was conducted with a non-parametric Wilcoxon rank sum test, $p<0.01$.

4.4 Evoked Oscillatory Responses were suppressed by inactivation of the MGm

With the MGm intact, each sound stimulus with the inter-stimulus-interval of 3 s evoked an oscillatory response in the auditory cortex. The same sound stimuli were less capable in triggering oscillatory responses when the MGm was inactivated. As shown in **Figure 23A,** when the MGm was intact, each stimulus evoked a sweep of oscillation. When the MGm was inactivated, sound stimuli-evoked oscillatory responses disappeared (**Figure 23A, B**). However, the spontaneous oscillatory activity that was not locked to the stimuli remained. The injection site was labeled with electrical lesion which was shown in **Figure 23C**. In the same preparation, a control experiment was conducted by inactivating MGv with which was also labeled.

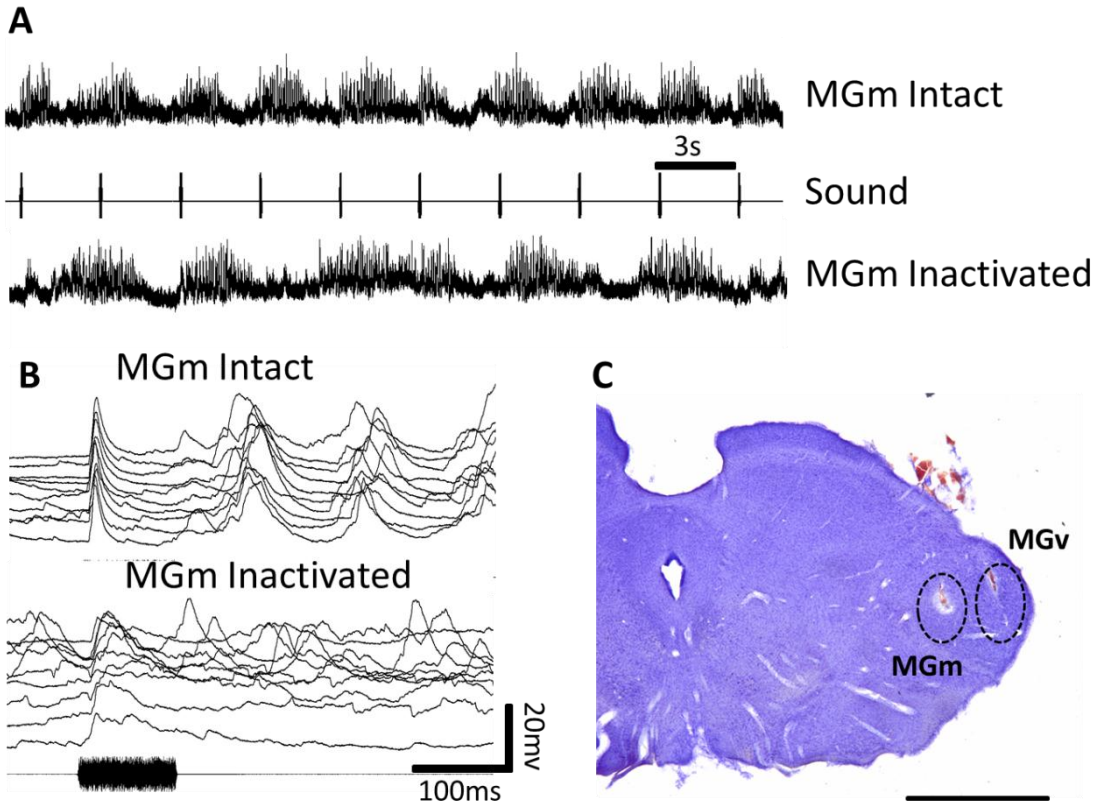

Figure 23 Inactivation of the MGm inhibits evoked oscillatory responses.

A, Comparison of raw intracellular Vm recordings before and after the inactivation of the MGm. In each acoustic stimulation cycle, a train of Vm fluctuations were evoked by a burst of noise of 100 ms duration while the MGm was intact. After inactivated the MGm, the oscillatory activity did not follow the acoustic stimuli was seemly spontaneously occurring.

B, Several trials of Vm recording aligned to the acoustic stimuli at an expanded time scale. Upper panel: evoked EPSPs consist with the onset part and a train of subsequent fluctuations. Lower panel: the onset of EPSPs exists, but the subsequent fluctuations are not evident and only spontaneous EPSPs remain.

C, Histological confirmation of the injection sites in a coronal section of the MGB. The MGm and the MGv are indicated with dotted ellipses in this Nissl stained section. Scale bar 2mm.

4.5 Sound Evoked EPSPs in cortical neurons were delayed by inactivation of the MGm

In extracellular, as well as intracellular recordings, delayed auditory responses were found. We measured the latencies of sound-evoked EPSPs with intracellular recordings. As shown in **Figure 24A**, sound evoked EPSPs were aligned according to the sound stimuli. The latency of EPSP onset was 9.5 ms when the MGm was intact and was 13.5 ms after the MGm was inactivated. Ten neurons from individual subjects in which the MGm was inactivated were included in the statistical analyses. The latency of EPSP onset was postponed from 15.1+/-1.07 ms to 19.6+/-1.84 ms (mean+/-SE, n=10,p=0.005, paired t-test).

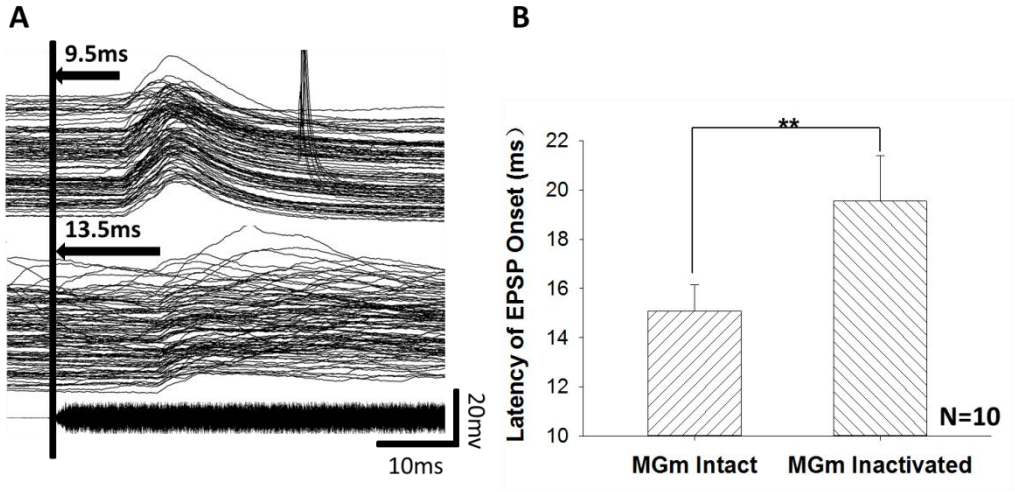

Figure 24 Inactivation of the MGm prolonged the onset time of EPSPs as shown by intracellular recordings.

A, EPSPs aligned according to the sound stimuli. The EPSP onset times were measured directly from aligned traces. In the present case, the EPSP onset time was 9.6 ms when the MGm was intact and 13.5 ms when the MGm was inactivated.

B, Group data indicating that EPSP onset time increased after the inactivation of the MGm. Means and standard errors of the EPSP onset times for 10 neurons before (left slash) and after(right slash) inactivation of the MGm are shown in histograms. A paired t-test was used for statistical analysis.

4.6 Inactivation of the MGv totally abolished the auditory responses of cortical neurons

As a control, we also inactivated the MGv and examined the auditory responses in the cortex. When the MGv was temporally inactivated, the extracellular spikes in response to the acoustic stimuli were totally abolished for a period of time (**Figure 25)**. The MGv is recognized as a driver of the AC, which carries the main stream of auditory inputs. Inactivation of the MGv should cut off the ascending auditory pathway. Although there were inputs from other ascending projections that remained, for instance, the input from the non-lemniscal MGm projections, these inputs were not strong enough to evoke visible extracellular responses. When the MGv recovered from its inactivated state, the auditory responses in the cortex reappeared.

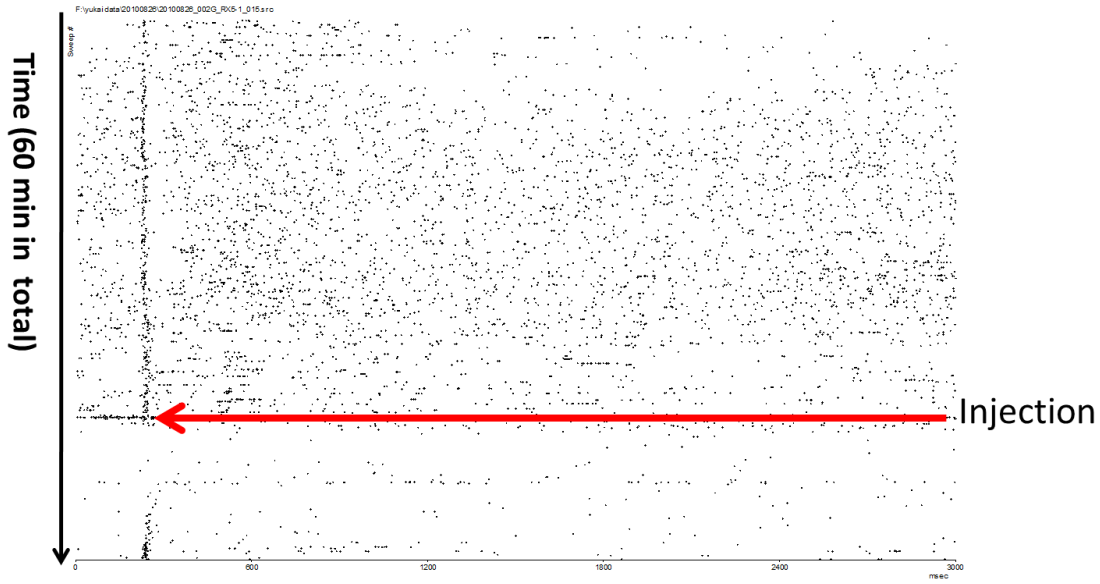

Figure 25 Inactivation of the MGv abolished the evoked responses in the auditory cortex. Raster plot showing the neuronal responses of the auditory cortex to acoustic stimuli. Injection of lidocaine (indicated by the red arrow) abolished the neuronal responses. After approximately 10 min, the auditory cortex recovered responses to acoustic stimuli.

4.7 Single cortical neuron can change the global state of auditory cortex

Further investigation into how the feed-forward modulation by the MGm modulates the state of cortical neurons. The MGm projects to layers I and VI of the cortex. Layer VI has been suggested to be the main origin of corticothalamic projections. Therefore, we focused on layer I. Cortical layer I is remarkable for its paucity of neurons and richness of dendritic profiles. A prominent feature of intrinsic layer I neurons is their horizontally developed dendrites in contrast to the vertical arrangement of dendrites in other layers. Taking advantage of intracellular recording, we artificially triggered burst firing in a single neuron from layer I. A short period (90s) of burst firing caused changes in the extracellular spikes and LFPs recorded at distal electrodes (**Figure 26**). Spontaneous membrane fluctuations were prominent in the intracellular recording, and corresponding activities in extracellular recordings and LFPs were present in the distal electrodes that were 1-2 mm away from the intracellular electrode. Burst firing depressed Vm fluctuations, as shown in the intracellular recordings, and also changed the extracellular activity and the LFP. Two successfully recorded neurons in the superficial layers showed impact in changing the global state of the cortex which were presented in **Figure 26**. We also performed the same manipulation of neurons of the deep layers (Layer IV or lower) of the auditory cortex: these manipulations did not alter global states (**Figure 27**). Some neurons were successfully labeled with neurobiotin, and their morphologies and locations in the cortex were shown in **Figure 28**.

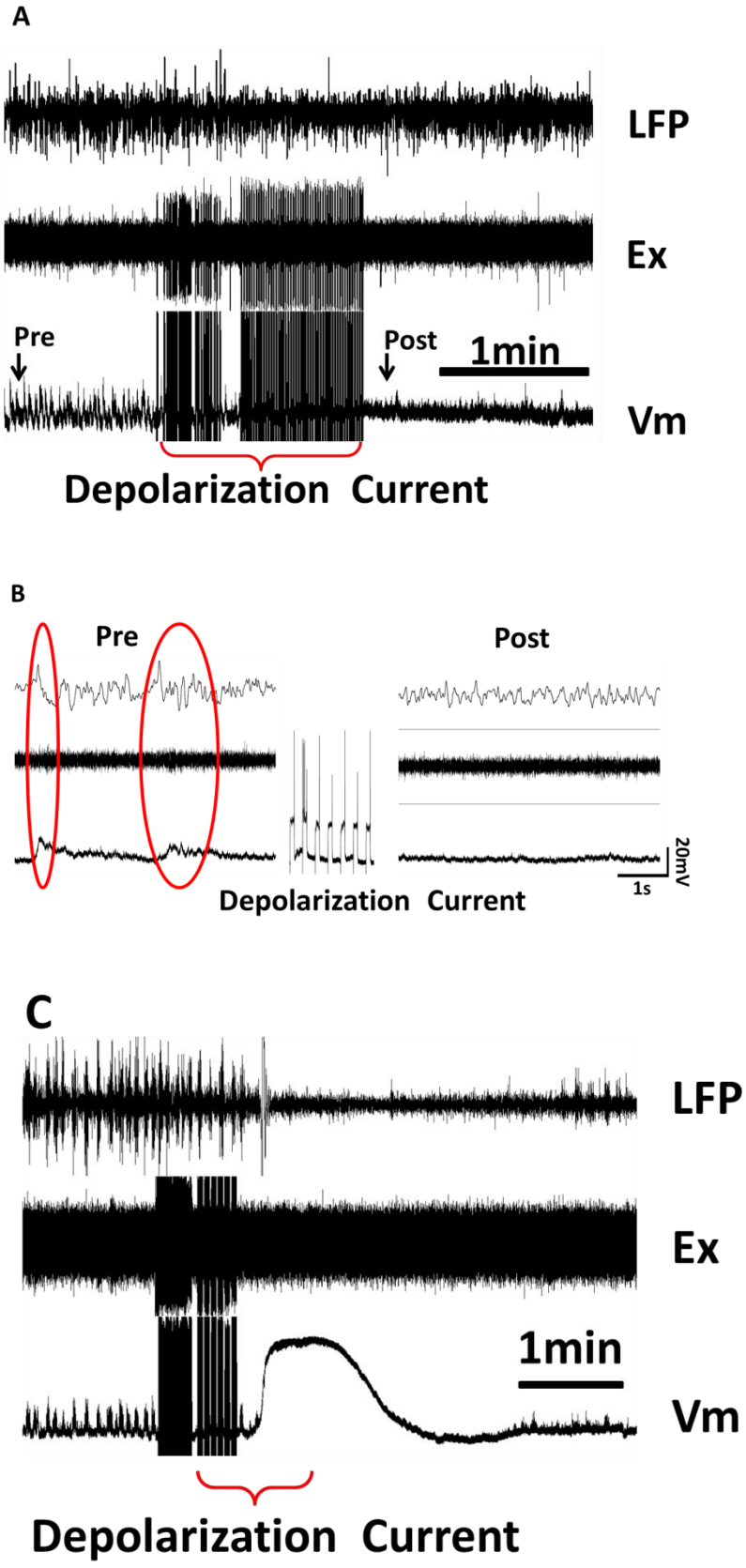

Figure 26 Firing of single cortical neurons change the global state of the auditory

cortex.

A, Simultaneous extracellular, local field potential (LFP), and intracellular recordings were performed in the auditory cortex. The distance between extracellular electrodes and intracellular electrodes was approximately 1 mm, and the distance from intracellular electrode to the LFP electrodes was approximately 2 mm.

Burst firings were triggered in the intracellularly recorded neuron by injecting depolarizing current (3Hz, 2 min in total). Spontaneous activity across all three channels decreased.

B, Comparison of spontaneous neuronal activities before and after manipulation of a single neuron on an expanded time scale. Synchronized activities are presented for three channels as indicated with ellipses before the manipulation.

C, Another case showing that the firing of a single cortical neuron caused a change in the spontaneous activity of the activated neuron, extracellular recording of the neighbouring neuron and a field potential from a distant electrode.

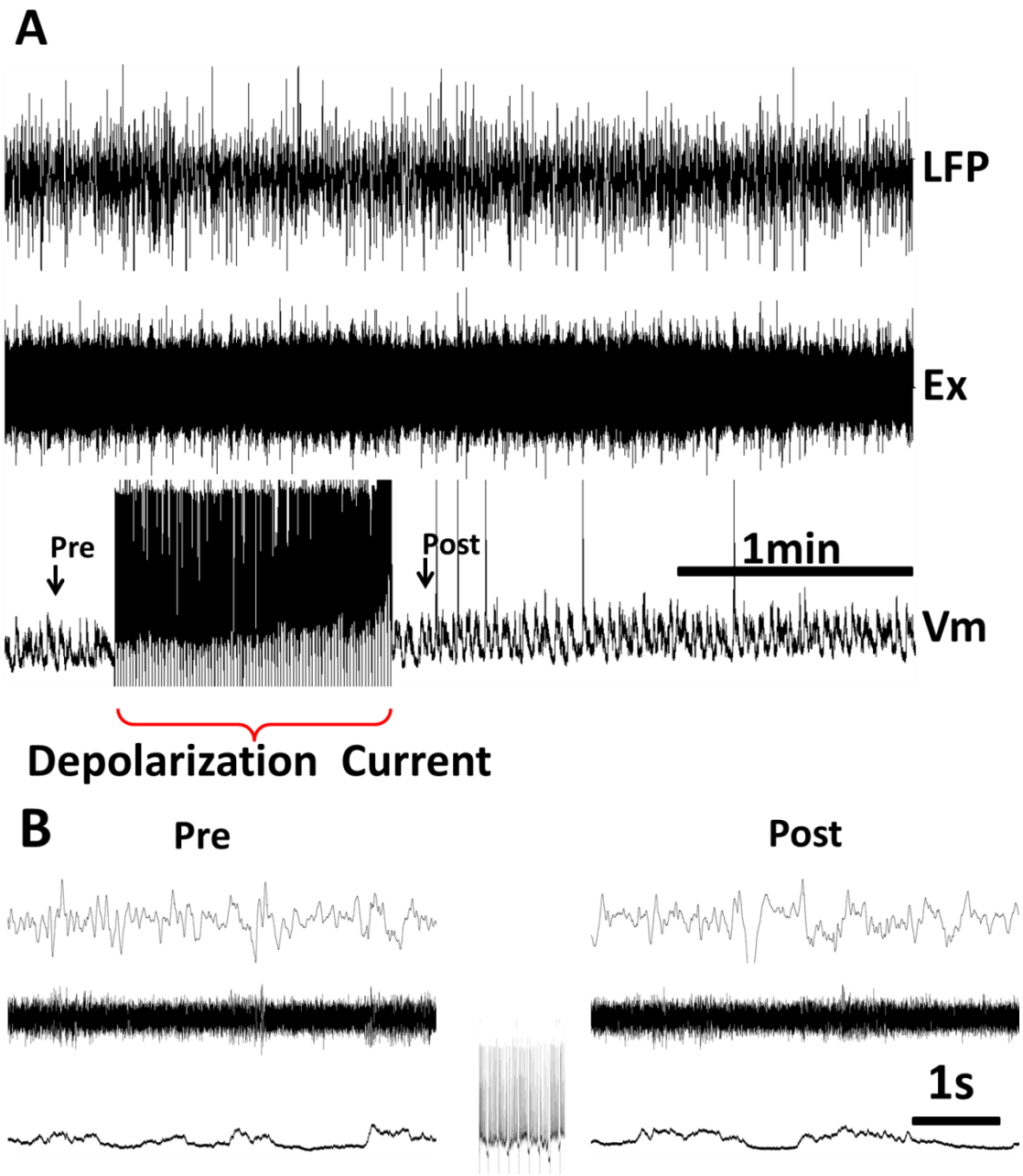

Figure 27 Long lasting burst firings of cortical neuron in the deep layer is not capable to change global state of cortex.

A, Simultaneous extracellular, local field potential (LFP), and intracellular recordings were performed in the auditory cortex. The distance between extracellular electrodes and intracellular electrodes was approximately 1 mm, and the distance from intracellular electrode to the LFP electrodes was approximately 2 mm. The depth of intracellular electrode was about 1mm below the pia matter.

B, Comparison of spontaneous neuronal activities before (pre) and after (post) manipulation of a single neuron on an expanded time scale.

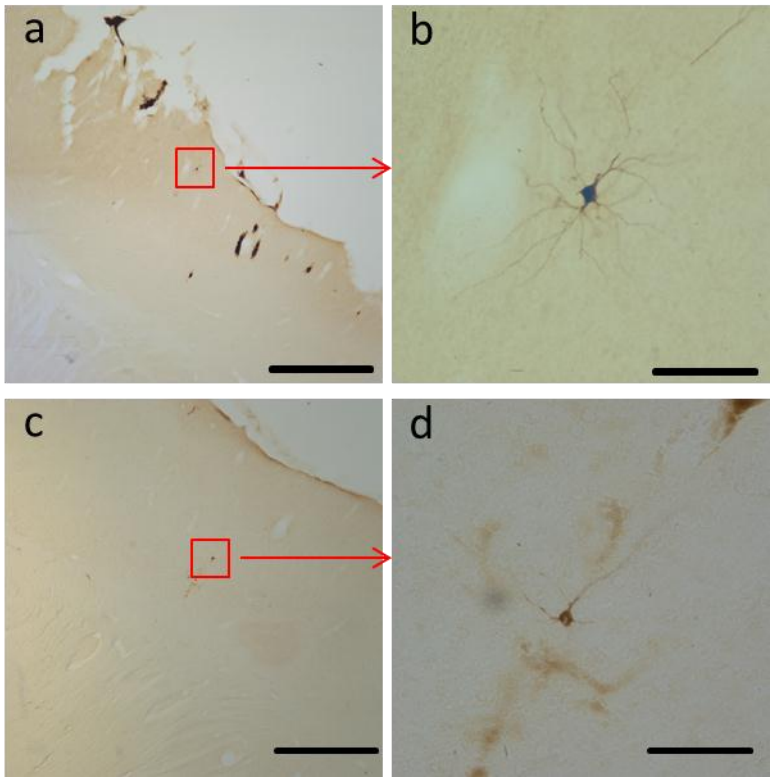

Figure 28 Histological confirmation that neurons were from the superficial and deep layers of the auditory cortex. Neurons are labeled with biocytin and stained with the DAB method. Figure A and B show a neuron in layer I. Figure C and D show a neuron in layer IV or V. Scale bar in A, C 1mm; in B, D 100um.

4.8 Discussion

In mammals, although the central auditory nervous systems exhibit diversity, the thalamocortical loops show highly similarity among species. In the present experiment, guinea pigs were chosen as subjection, as they had a large and flat auditory cortical area which was easy to access.

Lidocaine was used to temporally inactivate thalamic nuclei. As a widely used local anesthetic, it has moderate effective duration with a quick onset. From our experimental observations, the inactivation caused by lidocaine lasted from 10min to 30 min. So that we were able to conduct repeated measurements in the same preparation.

There were two observations in the present experiment:

(1) The delayed auditory response with the MGm inactivation;

(2) The changed sound evoked response pattern.

The increased response latencies were both found in the extracellular and intracellular recordings when the MGm was inactivated by injecting lidocaine. The extracellular spikes can be viewed as outputs of cortical neurons in response to the auditory stimuli. Onsets of EPSPs following auditory stimuli as shown in the intracellular recordings represented inputs to these neurons. Both of them could be seen as results of competing between stimulus evoked excitatory and inhibitory conductances. Disturbance to the balanced excitation and inhibition would change response latencies. As the MGm carried the fast auditory signal to the cortex, inactivation of the MGm disturbed the original balance, thereby caused increased latencies. Unlike the MGv which projects to Layers IV and III in the auditory cortex, the MGm projects mainly to Layer I. One target to Layer I projections is neurons in the superficial layers. It has been reported that most neurons in Layer I are GABAergic neurons. Another target of the Layer I projections is the abors of the apical dendrites of pyramidal neurons in deeper layers. The inactivation of the MGm influenced the responsiveness of the auditory cortex. In contrast, the inactivation of the MGv blocked the driving force of auditory signal from the thalamus to the cortex. Another prominent property of Layer projections is the laterally developed axonal trunks. When the MGm was inactivated, all the recordings in the auditory cortex exhibited changed responses. It seems that the modulatory effect of the MGm is global in the auditory cortex.

Sound evoked neural oscillation was observed in the anaesthetic subject. The oscillation was disassociated from acoustic stimulus while the MGm was inactivated by injecting lidocaine. However, the spontaneous oscillations retained in the cortex. There were two possible mechanisms underlying the change of response patterns in the auditory cortex, which were the excitability of cortex and synchrony of neruons. Firstly, the stimulus evoked oscillation was much easier to be found in the anaesthetic preparation in contrast to the alert subject. It was supposed to be related to

hyperactivities of inhibition in the brain. Inactivation of the MGm reduced feed-forward input into superficial layer I in the auditory cortex. In rats, most of neurons in the layer I of AI were found to be GABAergic neurons. Reduced inputs into layer I neurons caused decrease inhibition in the cortex, as result sound was less capable to trigger oscillatory responses when the MGm was inactivated. Second, feed-forward inputs from MGm to the AI played as synchronizer in governing responses of cortical neurons. The oscillations were synchronized neural acitivities in response to sound stimuli. With the MGm inactivation, interactions among dispersive inhibitory and excitatory inputs onto the cortical neurons eliminated the evoked oscillations.

Chapter 5 Neuroplasticity in the auditory cortex-investigation of CCK's facilitation of LTP induction in cortical neurons

In the second part of this study, we investigated how CCK facilitates LTP in cortical neurons. We used in vivo intracellular recordings of the auditory cortices of anaesthetized guinea pigs and in vitro whole cell patch clamp recordings in cell cultures of isolated rat cortical neurons.

5.1 CCK Facilitated LTP in the auditory cortex of anaesthetized guinea pigs

As shown in **Figure 29A** from an intracellular recording from the auditory cortex of an anaesthetized guinea pigs, the neuron responded to acoustic stimuli with an excitatory postsynaptic potential (EPSP). The subsequent 5 trials of responses before and at 4 and 10 mins after a 2-trial pairing of pre- and postsynaptic activities in the presence of CCK are depicted. Presynaptic activity was induced with an acoustic stimuli, and postsynaptic activity was induced with a depolarizing current injection into the recorded neuron. An increase in the EPSP was observed at 4 min after pairing compared with the baseline. The EPSP was further potentiated at 10 min after conditioned pairing. The averaged amplitude of the EPSPs increased to 8.6 mV at 4 min and 12.9 at 10 min after conditioning from the baseline of 4.3 mV before the conditioning .

The retention of this potentiation was examined at different time points after pairing in 6 neurons. The potentiation lasted as long as the recording was kept: 10 min (4 cells), 15 min (1 cell), 50 min (1 cell) and 110 min (1 cell) (**Figure 29B**). Normally the neurons showed stronger potentiations at 10 min than at 4 min after the pairing.

EPSPs increased significantly from 3.9+/- 1.6 to 5.1+/- 1.7 mV after 2-trial pairing of pre- and post-synaptic activities in the presence of CCK ($P<0.01$, $n=14$).

No synaptic strengthening was observed after simultaneous co-occurrence of presynaptic input and postsynaptic firing without local application of CCK in the auditory cortex of the anesthetized guinea pig (**Figure 29C**). Statistically, the change in the neuronal response after the pairings was not significant (4.2+/- 1.6 vs. 4.4+/-1.5 mv, n=11, P=0.178). The control experiment examined whether the neuronal responses to acoustic stimulus were changed after pairing of the presynaptic input and postsynaptic firings without CCK. No synaptic strengthening was observed after presynaptic stimulation and CCK application alone. The control experiment examined whether the neuronal responses to acoustic stimuli were altered after local application of CCK to the recording site and repeated acoustic stimuli of 2 trials. As shown in Fig. 4C, the amplitudes of the onset of the EPSPs were not significantly changed (4.0+/-1.7 mV vs. 3.7+/-1.7 mV, n=14, P = 0.331). No synaptic strengthening of the recorded neuron was observed after only postsynaptic activity in the presence of CCK (4.0+/-1.7 mv vs. 4.3+/-1.7 mV, n=12, P = 0.412).

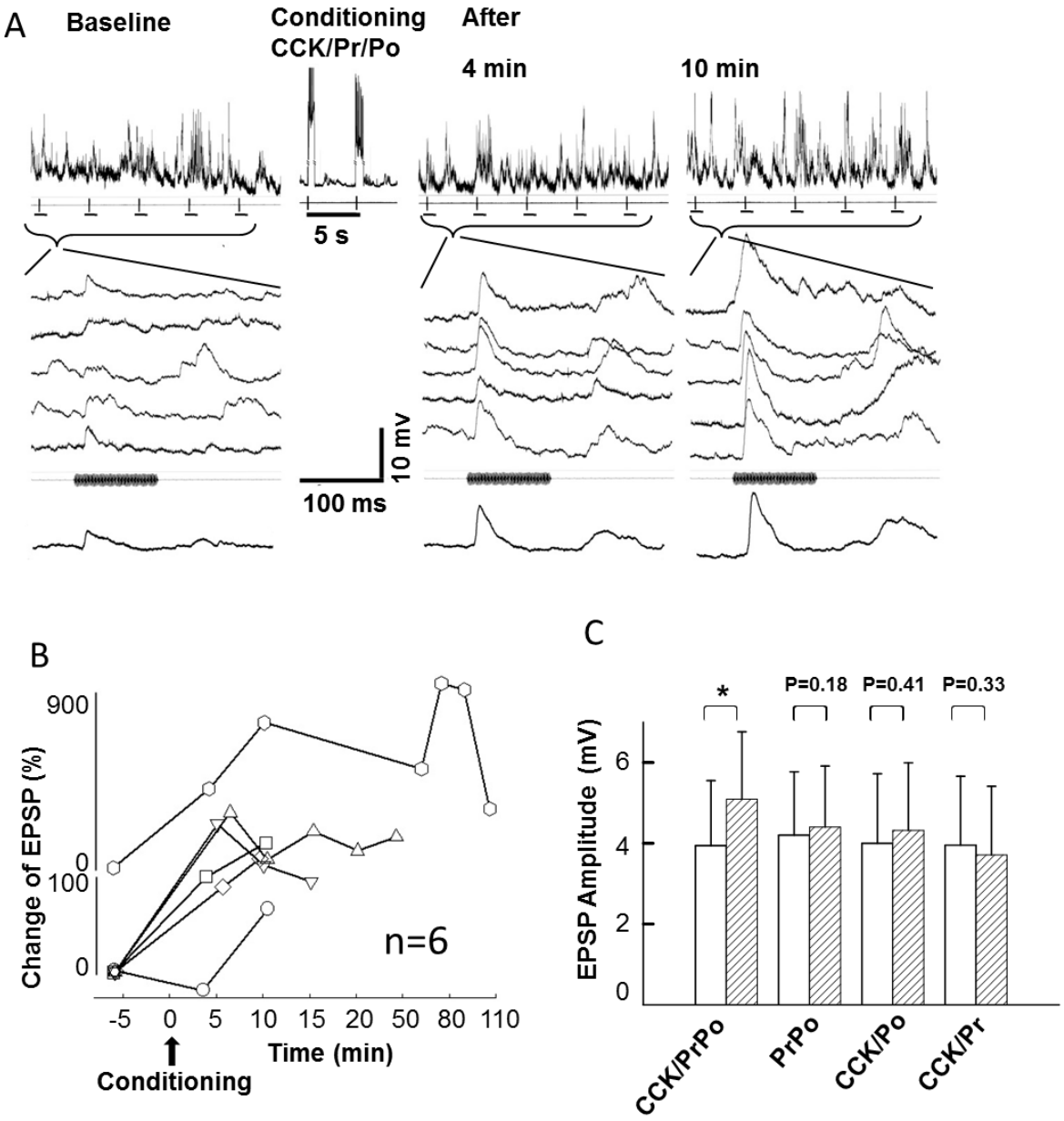

Figure 29 Long-term potentiation induced by 2-trial conditioning of paired pre- and post-synaptic activity after CCK application in the auditory cortex of an anesthetized guinea pig: in-vivo intracellular recording.

A, Neuronal responses to repeated acoustic stimuli before (baseline) and after the local application of CCK and conditioning: upper, the raw trace; middle, shows 5 consecutive individual trials; lower, the averaged traces. Conditioning was produced through depolarizing the recorded neuron for 400-600 ms that covered the acoustic stimuli.

B, The potentiation of the neuronal responses of 6 individual neurons was examined at different times after the above pairing.

C, Means and standard errors of the EPSP amplitudes before (open bars) and after (hashed bars) conditioning; controls are also shown. As the conditioning involved the following three elements: 1) CCK presence, 2) pre-synaptic input (auditory stimulus) and 3) post-synaptic activity (current injection that induced action potentials of the recorded neuron), it was abbreviated as CCK/PrPo. We adopted three controls, all of which included only two of the above three elements: PrPo, CCK/Po, and CCK/Pr (one of the examples is shown in Fig. 9B). * $P<0.05$, paired student's t-test.

We also examined whether electrically evoked EPSPs could be potentiated by CCK. Two metal electrodes were placed in the auditory cortex (**Figure 30A**). The electrical stimuli (ES) were adjusted to evoke small amplitude EPSPs in the recorded neuron (**Figure 30B**). Recordings were taken with ES applied alternatively on the two sides. However, conditioning pairing of ES and postsynaptic depolarizing current injection was only conducted for the left ES. After the conditioning pairing, the ES on the left side was of the same intensity as that evoked by the potentiated EPSPs. The amplitudes of evoked EPSPs in response to ES on the right remained unchanged.

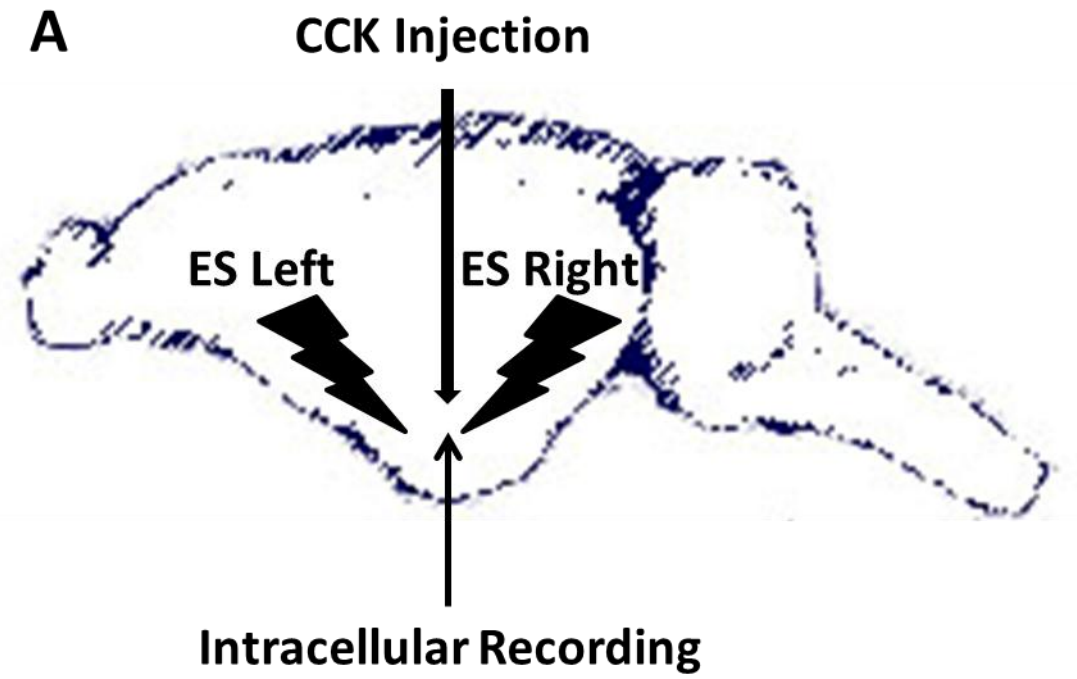

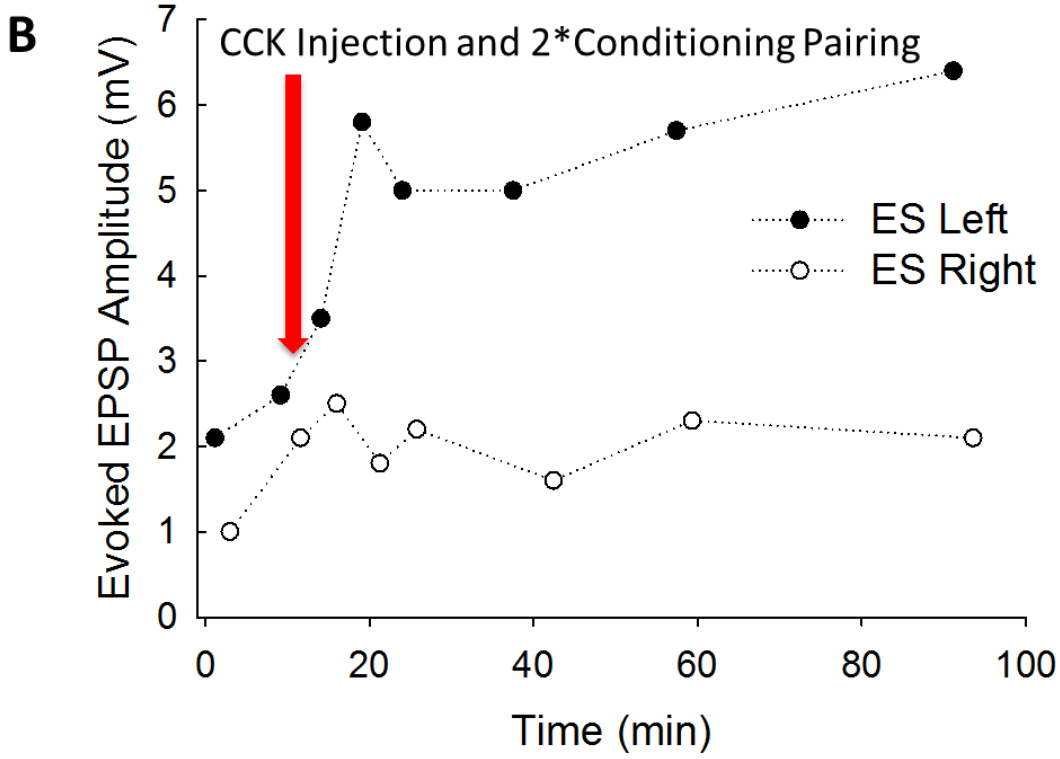

Figure 30 Electrically evoked potentials were potentiated after pairing with post-synaptic firing in the presence of CCK.

A, In the present experiment, electrical stimulation replaced the sound as the

pre-synaptic input. Two electrodes were placed 1 mm away from the intracellular electrode, one on the left and the other on the right. The electrical stimulation was a single depolarizing pulse with a width of 5 ms.

B, The 2-trial pairing of pre-synaptic electrical stimulation and post-synaptic depolarizing current injection in the presence of CCK successfully potentiated the electrically evoked potentials. The time of conditioning pairing and CCK injection is indicated by the arrow in the figure. As the conditioning pairing was only applied for the electrical stimuli on the left, evoked potentials by the right electrical stimuli remained unchanged.

Neurons in the primary cortex exhibited priority responsiveness to a single modality in normal conditions; for example, the neuron in the AI only responded to the acoustic stimulus. In the anaesthetized subject, visual stimulus (100ms white flash, with LED placed in front of the contralateral eye) was not capable to evoke visible response as shown in the intracellular recording. We found that the auditory neurons started to respond to the visual stimulus after it was paired with the depolarization for 40 trials (**Figure 31**). There were two successful recordings showing the potentiated visual responses after conditioning. The visual responses were both too weak to generate action potential, as there was no visual evoked spike observed.

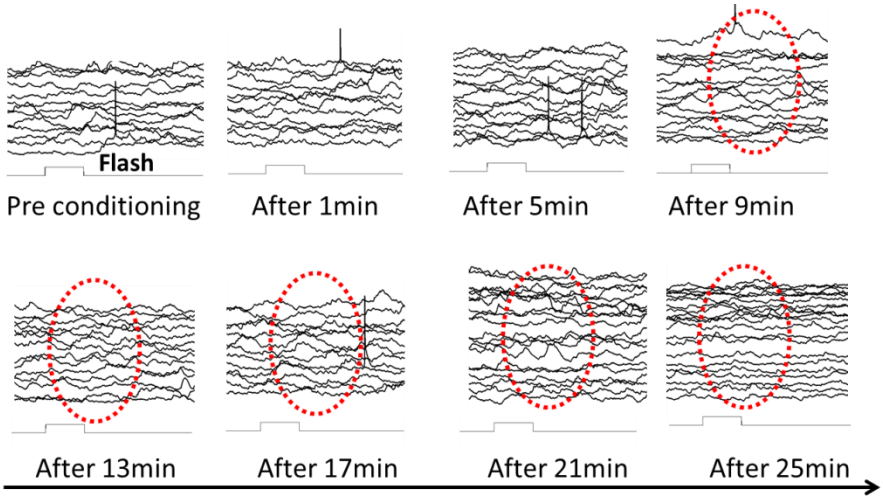

Figure 31 Visual responses in the auditory cortex as a result of conditioned pairing. There were no visible visual responses in the auditory cortex as shown in

pre-conditioning intracellular recording. The conditioned pairing consisted of 40 trials of visual stimulation(100 ms white flash) paired with depolarizing current injections. This auditory neuron started to respond to the visual stimulus approximately 9 minutes after the conditioned pairing. Weak EPSPs are visible in the aligned Vm recordings as indicated with dotted ellipses.

5.2 CCK Facilitated LTP in a Gradual Manner

In the presence of CCK, the cortex was capable of undergoing continuous plastic change as shown in the example **Figure 32A**. This neuron showed a shorter latency of onset EPSP at the first measurement after pairing (open arrowheads, t1 vs. t0). An inhibitory component was visible after the pairing (filled arrowhead, t1). The inhibition became stronger as time passed (filled arrowheads, t2-t4). Notably, the second EPSP increased and became stronger as time passed after the pairing (arrows, t0-t4).

Another example is shown in **Figure 32B**; the baseline was taken as $t_{0.}$ After puffing CCK, a fake conditioned pairing was conducted without the postsynaptic depolarization current injection, and the glutamate-activated EPSPs were also measured (time points after t1). Then, a second conditioned pairing that included pre-synaptic glutamate puffing and post-synaptic spikes was applied. The glutamate puffing activated EPSPs were measured at t2 to t4. The potentiated amplitudes of the EPSPs at t2 to t4 but not at t1 show that the post-synaptic spike was necessary to induce LTP in the presence of CCK.

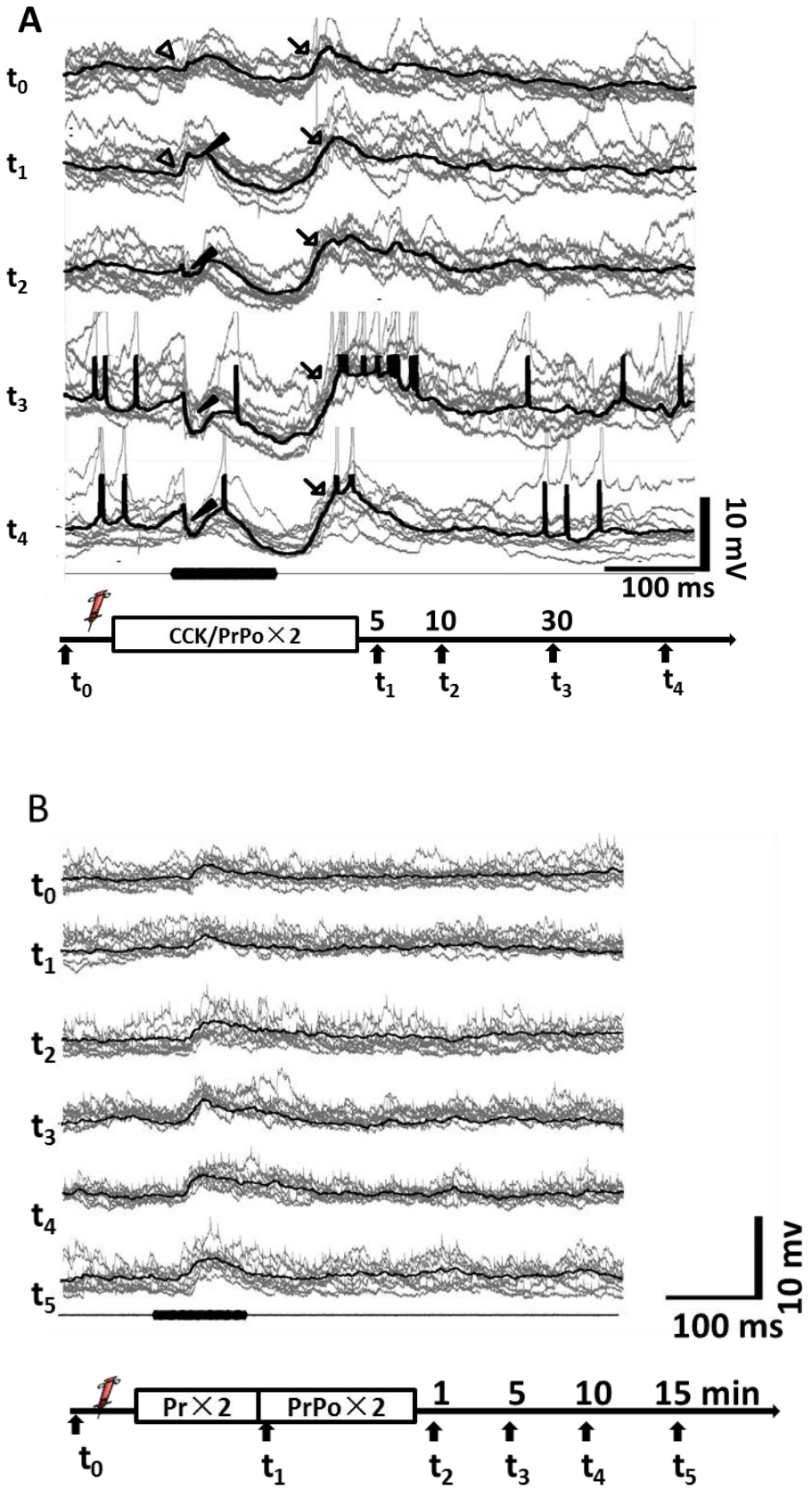

Figure 32 In-vivo intracellular recordings: time courses of evoked membrane

potentials after CCK injection in the auditory cortex of anesthetized guinea pigs.

A, Continuous change after CCK injection into the auditory cortex of an anesthetized guinea pig. The intracellular recordings show averaged responses (thick trace) and individual trial responses (gray traces) to the repeated delivery of auditory stimuli to the recorded neuron before (t0) and at different times (t1-t4) after the injection of CCK and the pairing of an auditory stimulus with current injection into the recorded neuron that triggered action potentials for 2 trials (CCK/PrPox2). Open arrowheads show the onset of EPSPs before and after the pairing (t0 and t1). Filled arrowheads show that an early inhibitory component appeared after the pairing at different times (t1-t4). Arrows show the second EPSP before and after the pairing (t0-t4). The experimental sequences and recording intervals are illustrated in the inset at the bottom. Scale bars apply to all traces.

B, Neuronal responses changed after the pairing of pre- and postsynaptic activities only in the presence of CCK. Traces show the neuronal responses (averaged, thick; individual trials, gray) to the conditioned stimulus before (t0) and after local application of CCK (t1-t5). The measurements (at t1) were carried out after a 2-trial presentation of the auditory stimulus (CCK/Prx2) while those at t2-t5 were carried out at different times after a further 2-trial presentation of the auditory stimulus and the depolarization of the recorded neuron (CCK/PrPox2) as shown in the experimental sequence at the bottom.

5.3 CCK Facilitated LTP in Cultured Cortical Neurons

To investigate the underlying mechanism of the facilitation of LTP by CCK, we switched to an in vitro approach in which we took whole cell recordings from cultured cortical neurons. As shown in **Figure 33**, the upper panel illustrates sample traces taken from a single neuron at the times indicated by the arrows, the amplitudes of glutamate activated EPSPs are plotted with dots and the bars represent the mean and SE. The experimental paradigm is illustrated on the bottom. The results from 5 neurons are included in the figure. From both the sample traces and the plot, we

conclude that the conditioned pairing that was conducted 20 s after the CCK puffing achieved potentiation, but the puffing conducted 120 s after CCK puffing did not.

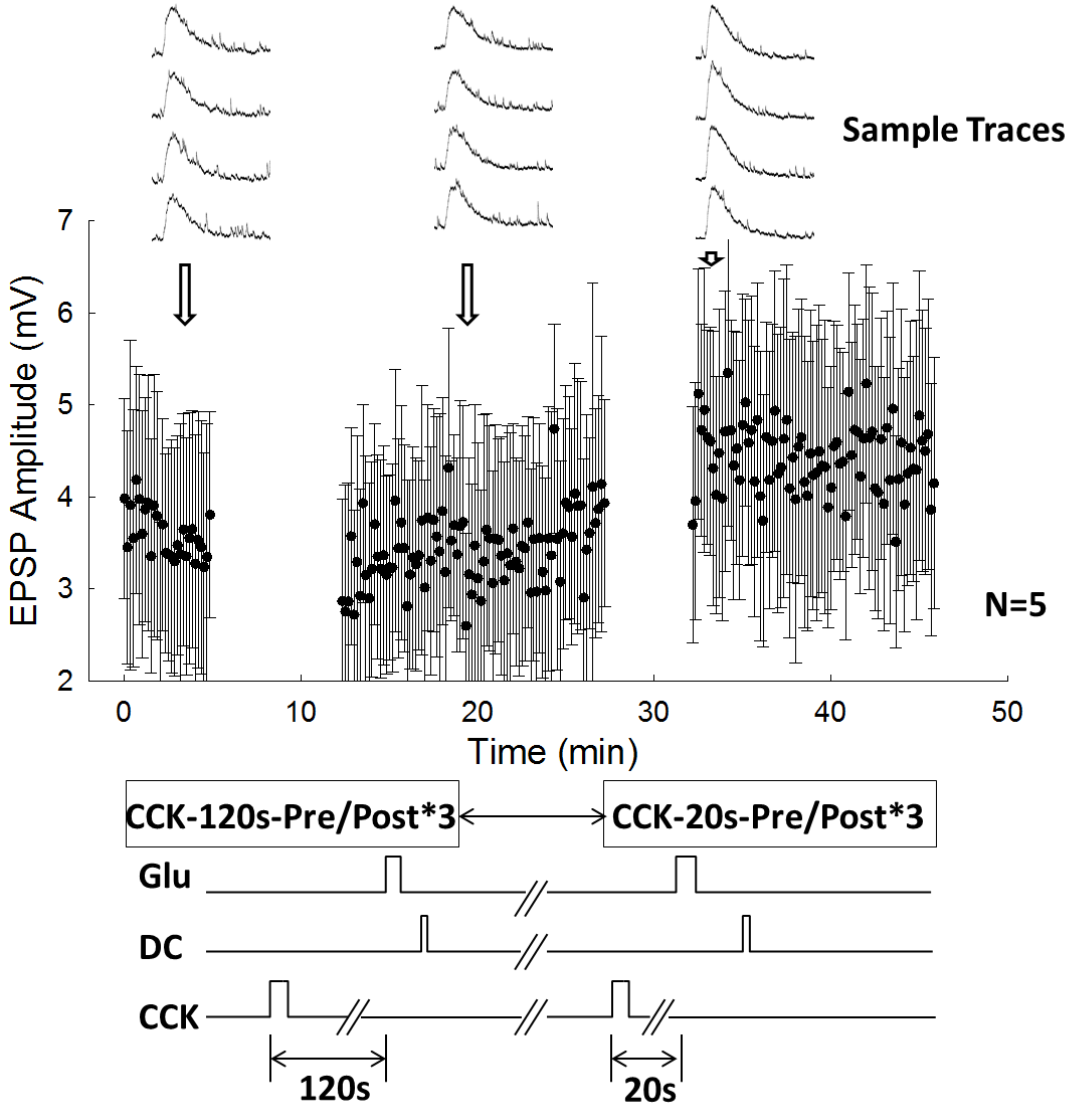

Figure 33 Glutamate-activated potentials that were potentiated only after a 3-trial pairing of glutamate puffing and postsynaptic depolarization shortly after CCK puffing. The experiment paradigm is illustrated at the bottom of the figure. The results from 5 neurons are presented. Means and standard errors of the glutamate-activated EPSP amplitudes for 5 neurons are plotted. In the first pairing, CCK puffing advanced the pairing by 120 s, and in the second pairing this advancement was 20 s. The EPSP amplitudes were only potentiated after the second pairing for each neuron. Sample traces are from one of the 5 neurons.

5.4 The Effective Time Window of CCK in Facilitating LTP

After verifying the facilitatory effect of CCK on LTP, we next investigated how CCK acted on cortical neurons. It is known that CCK binds to the CCKR, but the detailed mechanisms of this binding remain unclear. From a calcium imaging study of CHO cell cultures that inserted CCKBR, we learned that evoked calcium signals gradually vanish over 120s after the bath application of CCK (**Figure 34**). Thus, we next conducted experiments that involved conditioned pairings at different intervals after the puffing of CCK. All 8 neurons with conditioned pairing 20 s after the application of CCK exhibited potentiated EPSPs. In the 60 s group, 4 out 7 neurons showed potentiation. However, the remaining 3 neurons exhibited potentiated responses after the second conditioning paring that was conducted 20 s after the puffing of CCK (**Figure 35**). In contrast, all the 5 neurons that had conditioned pairing 120 s after the puffing of CCK did not show various potentiated EPSPs.

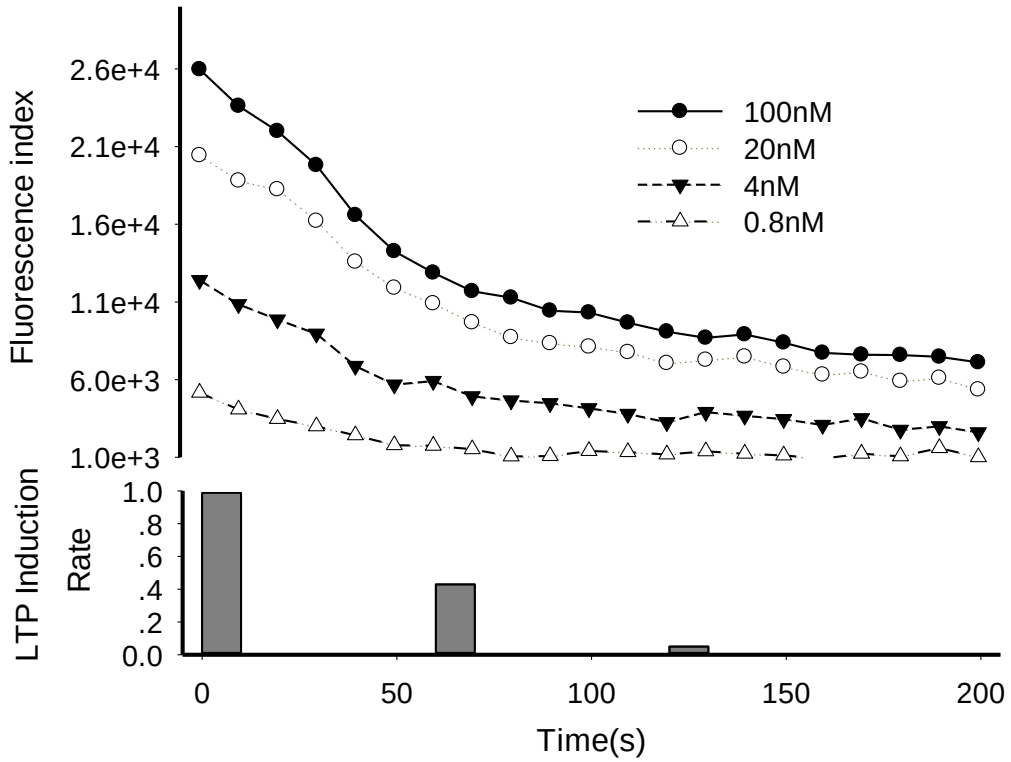

Figure 34 CCK receptor activation time window. In CHO cells transfected with CCKBR, CCK-8s was infused into the bath, which triggered calcium increases in the

cells. Fluorescent indices reflect the intracellular calcium concentrations, which became stable at approximately 120 s after CCK infusion. The time window of CCKBR activation in CHO cell agrees with the effective time window for CCK puffing in advance of conditioning pairing. The lower panel shows successful rates for LTP induction by puffing CCK at different times prior to the conditioning pairings. When CCK was puffed at 120 s before the conditioning pairing, no potentiation was observed(n=5), at 60 s 4 out of 7 neurons were potentiated, and at 20 s all 8 neurons showed potentiation.

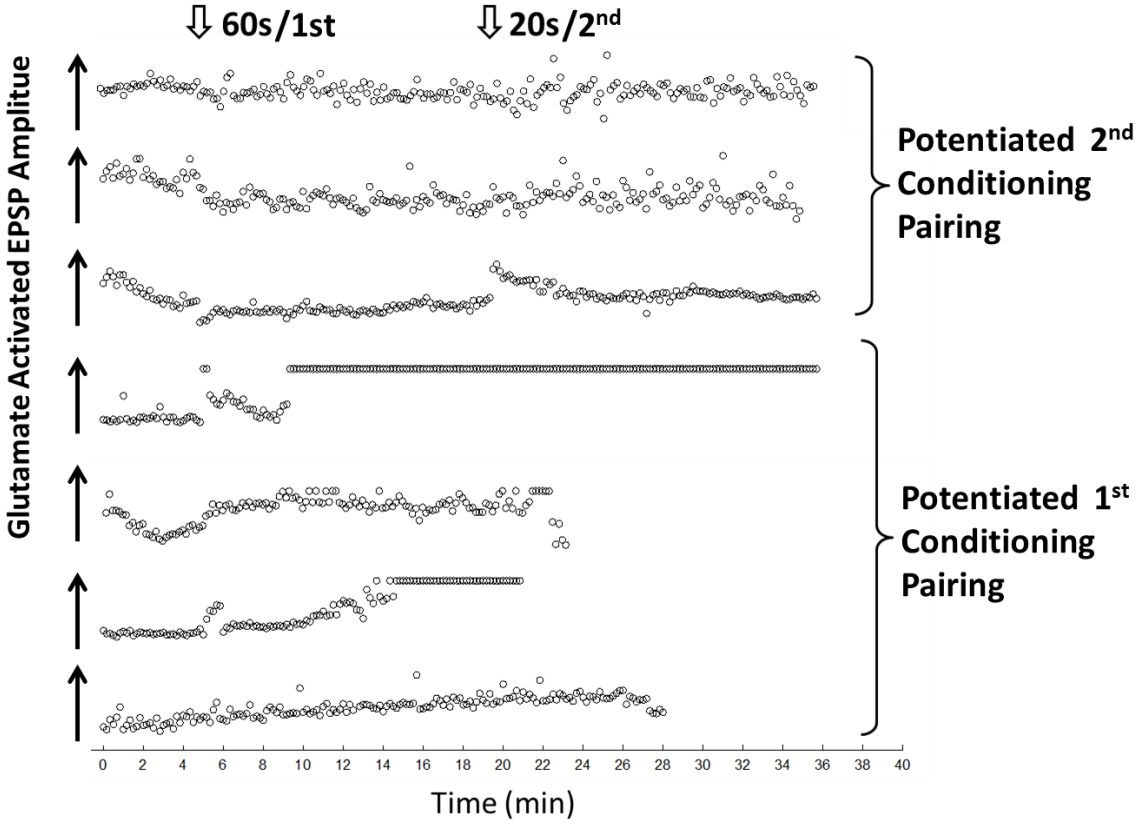

Figure 35 Glutamate activated EPSPs in some neurons were potentiated with CCK puffing 60 s before the conditioned pairing. From top to bottom results from 7 neurons are illustrated. For each neuron, conditioning pairing was enforced for the first 60s after CCK puffing. Four neurons exhibited potentiated responses to the same amount of glutamate puffing. As there were several action potentials from the neurons in response to the glutamate puffing, they were converted to EPSPs at 20 mV as

shown with the dots on the top of the forth and sixth plots. Another 3 neurons were subjected to a second conditioned pairing, which was enforced 20 s after CCK puffing. These neurons also showed potentiated responses afterward.

5.5 Discussion

CCK was found to facilitate LTP induction in the *in vivo* experiment with anaesthetized guinea pigs. LTP was induced by combining pre-synaptic stimulation (acoustic stimulation or electrical stimulation or visual stimulation) with a depolarizing current injection in the presence of CCK, and lasted as long as stable recordings kept. In most of the results, it lasted more than 10min. The LTPs were shown as potentiated EPSPs in response to acoustic stimulation, electrical stimulation and visual stimulation. Facilitation effect in inducing LTP by neural modulators has been found long before. As one of the most abundant neural modulators in the central nervous system, CCK attracted our special attention. CCK is highly expressed in the hippocampal complex and its corresponding receptor is rich in the cerebral cortex. According to a widely recognized model of memory, cerebral cortex is the ultimate site to store long term declarative memory and interplay between hippocampal complex and cerebral cortex is essential in generating long term declarative memory. One the other hand, the LTP is also widely accepted as cellular mechanism underlying long term memory. Here, we tried to provide an alternative hypothesis to illustrate long term declarative memory formation. The LTP induction protocol was different to the typical one used in most of LTP experiments. In a typical LTP experiment, the high frequency stimuli were used to induce LTP. However, it is still unclear whether the high frequency stimulation is necessary to induce LTP in the natural condition. Meanwhile, neural modulations which are abundant in an intact nervous system were ignored in those LTP studies. Pairing pre-synaptic input and post-synaptic action potential twice in the presence of CCK could successfully induced LTP, which might be closer to neutral status.

In the following *in vitro* experiment, the effective time window of the activation

of CCK receptor was tested. It has been reported that activation of CCK receptor would increase intracellular calcium concentration, which was also confirmed by testing calcium dependent fluorescence index in the CHO cell line inserted with CCKBR gene. We found that the effective time window of CCK receptor activation was about 20-90s, which was approximate to the calcium entry time. We speculated the correlation between CCK receptor activation and calcium concentration. In the *in vitro* experiment , glutamate puffing instead of real pre-synaptic input was used, glutamate evoked response was found to be potentiated after conditioning with CCK, so that a post-synaptical mechanism was speculated.

Chapter 6 Summary of findings and conclusions

In the present study, we showed that inactivation of the MGm causes a global state change in the auditory cortices of anaesthetized guinea pigs. The neuronal responses to auditory stimuli were delayed as manifested by the prolonged first spike latencies evidenced by the extracellular recordings and delayed EPSP onset times in the intracellular recordings. Furthermore, sound stimuli were less capable of triggering oscillatory responses in the auditory cortex when the MGm was inactivated. In contrast, inactivation of the MGv totally abolished the neuronal responses. As the MGm projects to layer I and layer VI, the neurons and neuropil in the superficial layer I and adjacent layer II are suggested as direct targets of thalamic modulation. We showed that the burst firing of single superficial cortical neurons are able to change neuronal activities at distant electrodes, suggesting a global impact.

Based on the present experimental data and previous evidence, we proposed a feed-forward thalamic modulation model (**Figure 36**). The thalamocortical projections contain a principal lemniscal part and a modulatory non-lemniscal part. The MGm belongs to the non-lemniscal part. It projects superficially to layer I of the cortex and interacts with neurons or neuropil and provides a feed-forward modulation of the neuronal responses to late-coming auditory signals that are transferred in the lemniscal projections. Neurons in the superficial layers (Layer I or II) have great potential to change the state of neurons over large areas. These neurons are suggested as candidates for the spreading of thalamic feed-forward modulation of the cortex.

Functional implication of the feed-forward thalamic modulation could be learnt by investigating other properties of neural responses, such as tuning curve, sound intensity threshold.

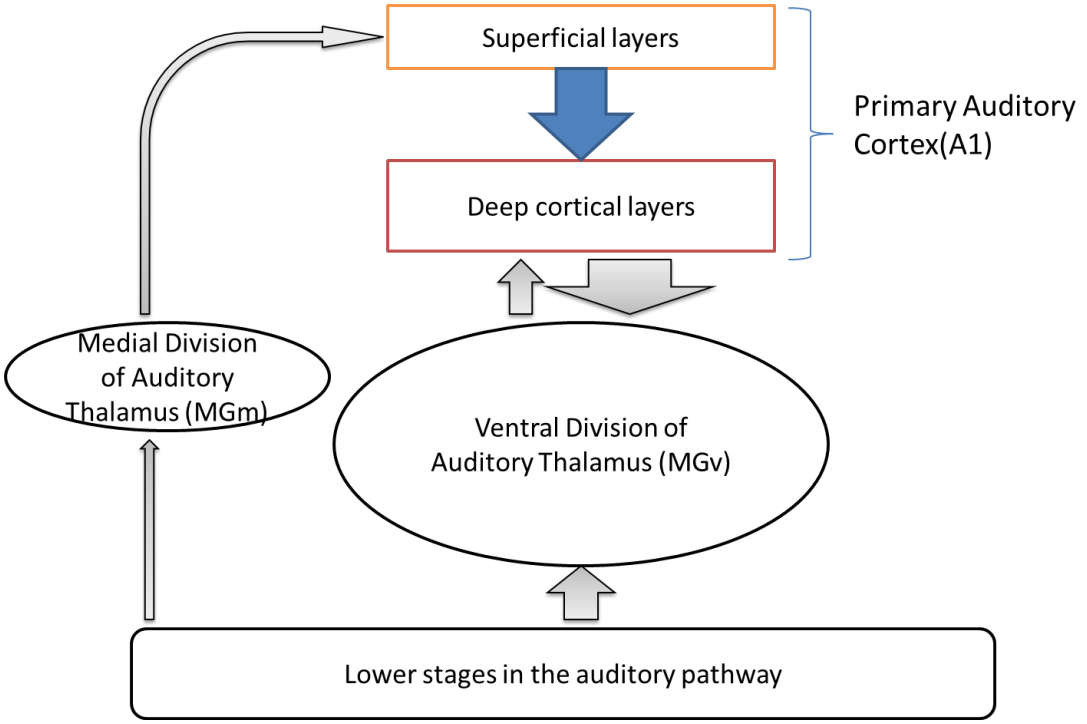

Figure 36 Feed-forward thalamic modulation system.

LTP is recognized as one of the most likely cellular mechanisms underlying memory function, and the neocortex is suggested to be the ultimate location for memory storage. In the present study, CCK was proven to facilitate cortical LTP induction in both in vivo and in vitro preparations. Long-term plasticity was induced through the pairing of pre- and post-synaptic neuronal activity after only 2 trials with local application of CCK in the auditory cortex of the anesthetized animal. The presence of CCK; presynaptic input and the firing of the postsynaptic neuron were the three prerequisites for inducing a change in synaptic strength. It has been suggested that CCK contributes to LTP induction through the G-protein coupled CCKBR. We suggest that the activation of CCKBR leads to elevation of calcium concentrations in post-synaptic neurons and triggers other secondary intracellular signals that facilitate neuronal plasticity. Morphological staining results from our lab have also shown that the neurons of the entorhinal and perirhinal cortices that project to the auditory cortex are CCK positive neurons that are capable of releasing CCK.

References：

Abeles, M. and M. H. Goldstein, Jr. (1970). "Functional architecture in cat primary auditory cortex: columnar organization and organization according to depth." J Neurophysiol **33**(1): 172-187.

Anderson, L. A. and J. F. Linden (2011). "Physiological differences between histologically defined subdivisions in the mouse auditory thalamus." Hear Res **274**(1-2): 48-60.

Beinfeld, M. C. (1985). "An overview of the biochemistry and anatomy of cholecystokinin (CCK) peptides in the brain." Prog Clin Biol Res **192**: 83-94.

Beinfeld, M. C. (2003). "Biosynthesis and processing of pro CCK: recent progress and future challenges." Life Sci **72**(7): 747-757.

Bi, G. Q. and M. M. Poo (1998). "Synaptic modifications in cultured hippocampal neurons: Dependence on spike timing, synaptic strength, and postsynaptic cell type." Journal of Neuroscience **18**(24): 10464-10472.

Bliss, T. V. and A. R. Gardner-Medwin (1973). "Long-lasting potentiation of synaptic transmission in the dentate area of the unanaestetized rabbit following stimulation of the perforant path." J Physiol **232**(2): 357-374.

Bliss, T. V. and T. Lomo (1973). "Long-lasting potentiation of synaptic transmission in the dentate area of the anaesthetized rabbit following stimulation of the perforant path." J Physiol **232**(2): 331-356.

Blum, P. S., M. J. Day, et al. (1979). "Thalamic components of the ascending vestibular system." Exp Neurol **64**(3): 587-603.

Chhatwal, J. P., A. R. Gutman, et al. (2009). "Functional interactions between endocannabinoid and CCK neurotransmitter systems may be critical for extinction learning." Neuropsychopharmacology **34**(2): 509-521.

Corkin, S., D. G. Amaral, et al. (1997). "H. M.'s medial temporal lobe lesion: findings from magnetic resonance imaging." J Neurosci **17**(10): 3964-3979.

Crawley, J. N., S. E. Hays, et al. (1981). "Neuropeptide modulation of social and exploratory behaviors in laboratory rodents." Peptides **2 Suppl 1**: 123-129.

Delfs, J. R. and M. A. Dichter (1985). "Cholecystokinin-octapeptide enhances synaptic activity in neurons cultured from rat cerebral cortex." Peptides **6 Suppl 1**: 139-144.

Desbois, C., P. Clerc, et al. (1998). "Differential tissular expression of the CCK(A) and CCK(B) gastrin receptor genes during postnatal development in the calf." Life Sci **63**(23): 2059-2070.

Diamond, D. M. and N. M. Weinberger (1984). "Physiological plasticity of single neurons in auditory cortex of the cat during acquisition of the pupillary conditioned response: II. Secondary field (AII)." Behav Neurosci **98**(2): 189-210.

Dockray, G. J. (1976). "Immunochemical evidence of cholecystokinin-like peptides in brain." Nature **264**(5586): 568-570.

Dockray, G. J. (2012). "Cholecystokinin." Curr Opin Endocrinol Diabetes Obes **19**(1): 8-12.

Dufresne, M., C. Seva, et al. (2006). "Cholecystokinin and gastrin receptors." Physiol Rev **86**(3): 805-847.

Fallon, J. H. and K. B. Seroogy (1984). "Visual and auditory pathways contain cholecystokinin: evidence from immunofluorescence and retrograde tracing." Neurosci Lett **45**(1): 81-87.

Flood, J. F. and J. E. Morley (1989). "Cholecystokinin receptors mediate enhanced memory retention produced by feeding and gastrointestinal peptides." Peptides **10**(4): 809-813.

Fuenzalida, M., D. Fernandez de Sevilla, et al. (2010). "Role of AMPA and NMDA receptors and back-propagating action potentials in spike timing-dependent plasticity." J Neurophysiol **103**(1): 47-54.

Gentile, B. F. and B. Miller (2009). Foundations of psychological thought : a history of psychology. Los Angeles, Sage Publications, Inc.

Glendenning, K. K., J. K. Brunso-Bechtold, et al. (1981). "Ascending auditory afferents to the nuclei of the lateral lemniscus." J Comp Neurol **197**(4):

673-703.

Graham, J. (1977). "An autoradiographic study of the efferent connections of the superior colliculus in the cat." J Comp Neurol **173**(4): 629-654.

Greenwood, R. S., S. E. Godar, et al. (1981). "Cholecystokinin in hippocampal pathways." J Comp Neurol **203**(3): 335-350.

Hammond, C., D. Paupardin-Tritsch, et al. (1987). "Cholecystokinin induces a decrease in Ca2+ current in snail neurons that appears to be mediated by protein kinase C." Nature **325**(6107): 809-811.

He, J. (1997). "Modulatory effects of regional cortical activation on the onset responses of the cat medial geniculate neurons." J Neurophysiol **77**(2): 896-908.

He, J. (2001). "On and off pathways segregated at the auditory thalamus of the guinea pig." J Neurosci **21**(21): 8672-8679.

Hebb, D. O. (1949). The organization of behavior; a neuropsychological theory. New York,, Wiley.

Henkel, C. K. (1983). "Evidence of sub-collicular auditory projections to the medial geniculate nucleus in the cat: an autoradiographic and horseradish peroxidase study." Brain Res **259**(1): 21-30.

Honda, T., E. Wada, et al. (1993). "Differential Gene Expression of CCK(A) and CCK(B) Receptors in the Rat Brain." Mol Cell Neurosci **4**(2): 143-154.

Hu, B. (2003). "Functional organization of lemniscal and nonlemniscal auditory thalamus." Exp Brain Res **153**(4): 543-549.

Ingram, S. M., R. G. Krause, 2nd, et al. (1989). "Neuronal localization of cholecystokinin mRNA in the rat brain by using in situ hybridization histochemistry." J Comp Neurol **287**(2): 260-272.

Ito, M. and M. Kano (1982). "Long-lasting depression of parallel fiber-Purkinje cell transmission induced by conjunctive stimulation of parallel fibers and climbing fibers in the cerebellar cortex." Neurosci Lett **33**(3): 253-258.

Jones, E. G. (2001). "The thalamic matrix and thalamocortical synchrony." Trends

Neurosci **24**(10): 595-601.

Katsuura, G. and S. Itoh (1986). "Preventive effect of cholecystokinin octapeptide on experimental amnesia in rats." Peptides **7**(1): 105-110.

Krupa, D. J., J. K. Thompson, et al. (1993). "Localization of a memory trace in the mammalian brain." Science **260**(5110): 989-991.

Kudo, M. and K. Niimi (1980). "Ascending projections of the inferior colliculus in the cat: an autoradiographic study." J Comp Neurol **191**(4): 545-556.

Lee, C. C. and J. A. Winer (2008). "Connections of cat auditory cortex: III. Corticocortical system." J Comp Neurol **507**(6): 1920-1943.

Lee, S. Y. and I. Soltesz (2011). "Cholecystokinin: a multi-functional molecular switch of neuronal circuits." Dev Neurobiol **71**(1): 83-91.

Li, C. Y., J. T. Lu, et al. (2004). "Bidirectional modification of presynaptic neuronal excitability accompanying spike timing-dependent synaptic plasticity." Neuron **41**(2): 257-268.

Lindefors, N., S. Brene, et al. (1991). "Distribution of cholecystokinin mRNA and peptides in the human brain." Neuroscience **42**(3): 813-821.

Meek, J. L., M. J. Iadarola, et al. (1983). "Cholecystokinin turnover in brain." Brain Res **276**(2): 375-378.

Mercer, L. D., P. M. Beart, et al. (1996). "On the distribution of cholecystokinin B receptors in monkey brain." Brain Res **738**(2): 313-318.

Miller, K. K., A. Hoffer, et al. (1997). "Cholecystokinin increases GABA release by inhibiting a resting K+ conductance in hippocampal interneurons." J Neurosci **17**(13): 4994-5003.

Mitani, A., K. Itoh, et al. (1984). "Thalamocortical projections to layer I of the primary auditory cortex in the cat: a horseradish peroxidase study." Brain Res **310**(2): 347-350.

Miyoshi, R., S. Kito, et al. (1991). "Cholecystokinin increases intracellular Ca2+ concentration in cultured striatal neurons." Neuropeptides **18**(3): 115-119.

Morris, R. G., P. Garrud, et al. (1982). "Place navigation impaired in rats with

hippocampal lesions." Nature **297**(5868): 681-683.

Nadol, J. B., Jr. (1983). "Serial section reconstruction of the neural poles of hair cells in the human organ of Corti. I. Inner hair cells." Laryngoscope **93**(5): 599-614.

Peters, A., M. Miller, et al. (1983). "Cholecystokinin-like immunoreactive neurons in rat cerebral cortex." Neuroscience **8**(3): 431-448.

Popper, A. N. and R. R. Fay (1992). The Mammalian auditory pathway : neurophysiology. New York, Springer-Verlag.

Purves, D. (2004). Neuroscience. Sunderland, Mass., Sinauer Associates, Publishers.

Rapisarda, C. and B. Bacchelli (1977). "The brain of the guinea pig in stereotaxic coordinates." Arch Sci Biol (Bologna) **61**(1-4): 1-37.

Scannell, J. W., G. Burns, et al. (1999). "The connectional organization of the cortico-thalamic system of the cat." Cerebral Cortex **9**(3): 277-299.

Schofield, B. R. and S. D. Motts (2009). "Projections from auditory cortex to cholinergic cells in the midbrain tegmentum of guinea pigs." Brain Res Bull **80**(3): 163-170.

Schreiner, C. E. and J. V. Urbas (1988). "Representation of amplitude modulation in the auditory cortex of the cat. II. Comparison between cortical fields." Hear Res **32**(1): 49-63.

Scoville, W. B. and B. Milner (1957). "Loss of recent memory after bilateral hippocampal lesions." J Neurol Neurosurg Psychiatry **20**(1): 11-21.

Seroogy, K. B., N. Brecha, et al. (1985). "Distribution of cholecystokinin-like immunoreactivity in the rat main olfactory bulb." J Comp Neurol **239**(4): 373-383.

Shinohara, S. and K. Kawasaki (1997). "Electrophysiological changes in rat hippocampal pyramidal neurons produced by cholecystokinin octapeptide." Neuroscience **78**(4): 1005-1016.

Sousa-Pinto, A., M. Paula-Barbosa, et al. (1975). "A Golgi and electron microscopical study of nerve cells in layer I of the cat auditory cortex." Brain Res **95**(2-3): 443-458.

Spoendlin, H. (1972). "Innervation densities of the cochlea." Acta Otolaryngol **73**(2): 235-248.

Squire, L. R., D. G. Amaral, et al. (1989). "Description of brain injury in the amnesic patient N.A. based on magnetic resonance imaging." Exp Neurol **105**(1): 23-35.

Squire, L. R., F. Haist, et al. (1989). "The neurology of memory: quantitative assessment of retrograde amnesia in two groups of amnesic patients." J Neurosci **9**(3): 828-839.

Steriade, M., E. G. Jones, et al. (1997). Thalamus. Amsterdam ; New York, Elsevier.

Sweatt, J. D. (2003). Mechanisms of memory. San Diego, Calif., Academic Press.

Thomson, A. M. and A. P. Bannister (2003). "Interlaminar connections in the neocortex." Cerebral Cortex **13**(1): 5-14.

Vanderhaeghen, J. J., F. Lotstra, et al. (1980). "Immunohistochemical localization of cholecystokinin- and gastrin-like peptides in the brain and hypophysis of the rat." Proc Natl Acad Sci U S A **77**(2): 1190-1194.

Vanderhaeghen, J. J., J. C. Signeau, et al. (1975). "New peptide in the vertebrate CNS reacting with antigastrin antibodies." Nature **257**(5527): 604-605.

Vigna, S. R., J. L. Morgan, et al. (1984). "Localization and characterization of gastrin/cholecystokinin-like immunoreactivity in the central nervous system of Aplysia californica." J Neurosci **4**(5): 1370-1377.

Wallace, M. N., R. G. Rutkowski, et al. (2000). "Identification and localisation of auditory areas in guinea pig cortex." Exp Brain Res **132**(4): 445-456.

Wang, S., A. P. Zhang, et al. (2011). "Cholecystokinin facilitates neuronal excitability in the entorhinal cortex via activation of TRPC-like channels." J Neurophysiol **106**(3): 1515-1524.

Webster, D. B., A. N. Popper, et al. (1992). The Mammalian auditory pathway : neuroanatomy. New York, Springer-Verlag.

Weinberger, N. M. (2011). "The medial geniculate, not the amygdala, as the root of auditory fear conditioning." Hear Res **274**(1-2): 61-74.

Whitley, J. M. and C. K. Henkel (1984). "Topographical organization of the inferior collicular projection and other connections of the ventral nucleus of the lateral lemniscus in the cat." J Comp Neurol **229**(2): 257-270.

Willetts, J., L. Urban, et al. (1985). "Actions of cholecystokinin octapeptide on rat spinal dorsal horn neurons." Ann N Y Acad Sci **448**: 385-402.

Winer, J. A. (1984). "The human medial geniculate body." Hear Res **15**(3): 225-247.

Winer, J. A. (1984). "Identification and structure of neurons in the medial geniculate body projecting to primary auditory cortex (AI) in the cat." Neuroscience **13**(2): 395-413.

Winer, J. A. (1985). "The medial geniculate body of the cat." Adv Anat Embryol Cell Biol **86**: 1-97.

Winer, J. A. (1986). "Neurons accumulating [3H]gamma-aminobutyric acid (GABA) in supragranular layers of cat primary auditory cortex (AI)." Neuroscience **19**(3): 771-793.

Winer, J. A., J. J. Diehl, et al. (2001). "Projections of auditory cortex to the medial geniculate body of the cat." J Comp Neurol **430**(1): 27-55.

Winer, J. A. and D. T. Larue (1989). "Populations of GABAergic neurons and axons in layer I of rat auditory cortex." Neuroscience **33**(3): 499-515.

Winer, J. A., L. M. Miller, et al. (2005). "Auditory thalamocortical transformation: structure and function." Trends in Neurosciences **28**(5): 255-263.

Xiong, Y., Y. Q. Yu, et al. (2004). "Effects of cortical stimulation on auditory-responsive thalamic neurones in anaesthetized guinea pigs." J Physiol **560**(Pt 1): 207-217.

Yang, Y. M., J. M. Chung, et al. (2006). "Cellular action of cholecystokinin-8S-mediated excitatory effects in the rat periaqueductal gray." Life Sci **79**(18): 1702-1711.

Zhao, H., D. C. Kinch, et al. (2011). "Pharmacological investigations of the cellular transduction pathways used by cholecystokinin to activate nodose neurons." Auton Neurosci **164**(1-2): 20-26.

Zola-Morgan, S. and L. R. Squire (1993). "Neuroanatomy of memory." Annu Rev Neurosci **16**: 547-563.

Zola-Morgan, S., L. R. Squire, et al. (1986). "Human amnesia and the medial temporal region: enduring memory impairment following a bilateral lesion limited to field CA1 of the hippocampus." J Neurosci **6**(10): 2950-2967.

Zola-Morgan, S., L. R. Squire, et al. (1994). "Severity of memory impairment in monkeys as a function of locus and extent of damage within the medial temporal lobe memory system." Hippocampus **4**(4): 483-495.